Modified GLRT Demodulation for OFDM Signal Transmitted Over a Frequency-Selective Fading Channel

Prepared by Hsin-Yu Kuo

Advisory by Prof. Po-Ning Chen

In Partial Fulfillment of the Requirements

For the Degree of Master of Science

Institute of Communications Engineering

National Chiao Tung University

Hsinchu, Taiwan 300, R.O.C.

E-mail: uyuni508@gmail.com

June, 2011

Abstract

In this thesis, we propose the so-called Modified GLRT demodulator for combined channel estimation and data correction for OFDM signals transmitted over a frequency selective channel with unknown channel coefficients. Simulation results confirm that the Modified GLRT can achieve an evidently better performance than the traditional GLRT. In order to reduce the demodulation complexity, we further derive the recursive metric formula based on the Modified GLRT criterion for use of the priority-first search algorithm. This results in a much lower demodulation complexity in comparison with the exhaustive demodulator.

Acknowledgements

I would like to express my gratitude to my advisor, Prof. Po-Ning Chen. My gratitude also goes to Dr. Chia-Lung Wu and those who have made this thesis possible. Finally, I would like to dedicate this thesis to my family, for their support and love.

Contents

List of Figures

Chapter 1

Introduction

1.1 Overview

Orthogonal frequency-division multiplexing (OFDM) is an effective multicarrier technique for wireless systems over the frequency selective channel [1]. Conventionally, a typical receiver for wireless communication system performs channel estimation, channel equalization and data detection separately. However in recent researches [2][3], the demodulator combined channel estimation and data detection has been considered a promising approach to combat the effects of multi-path fading. The demodulation is regarded as blind because the channel fading coefficients are unknown to both the receiver and transmitter. According to [3][4], the generalized likelihood ratio test (GLRT) is the best decision maker for blind demodulation.

In this thesis, we develop a blind demodulator, termed as the Modified GLRT, for an OFDM system transceived over a frequency selective channel with unknown channel coefficients. In short, it jointly performs the channel estimation and data correction. In order to reduce the demodulation complexity, a priority-first search demodulation algorithm as well as the recursive metric formula used by this algorithm is also proposed.

We organize the thesis as follows. Chapter 2 gives the necessary background for the noncoherent OFDM system, GLRT demodulation and prority-first search algorithm. Chapter

3 introduces the Modified GLRT demodulator we propose, and derive the recursive metric for its corresponding priority-first search demodulator. Chapter 4 presents and remarks the simulation results. Chapter 5 concludes the thesis.

1.2 Acronyms and Notations

Some acronyms and common identifiers used in this thesis are listed below.

OFDM orthogonal frequency division multiplexing

AWGN additive white Gaussian noise

PSK phase shift keying

DFT discrete Fourier transform

GLRT general likelihood ratio test

ModGLRT modified general likelihood ratio test

BER bit error rate

ML maximum-likelihood

SNR signal-to-noise ratio

Symbol	Meaning
$\boldsymbol{x}$	a time domain vector *(The following notations are simple representative examples. Similar notations are applied to other alphabets.)*
$\boldsymbol{X}$	a frequency domain vector
$\mathbb{Q}$	a matrix
X_k	the k-th component of a vector $\boldsymbol{X}$
$Q_{k,\ell}$	the element of a matrix $\mathbb{Q}$ at row k and column ℓ
$\|\boldsymbol{X}\|^2$	the norm of a vector $\boldsymbol{X}$
$\boldsymbol{X}^T$	transpose of a vector $\boldsymbol{X}$
$\boldsymbol{X}^\dagger$	Hermitian transpose operation of a vector $\boldsymbol{X}$
$\texttt{trace}(\mathbb{Q})$	the trace of a square matrix $\mathbb{Q}$
$\texttt{vec}(\mathbb{Q})$	the operation to transform a matrix into a vector

Chapter 2

Technical Background

In this chapter, the background knowledges about the orthogonal frequency division multiplexing (OFDM) system, the general likelihood ratio test (GLRT) and the maximum-likelihood priority-first search demodulation/decoding algorithm are provided. Specifically, we first introduce the non-coherent OFDM system in Section 2.1 [6]. We then present in Section 2.2 the GLRT criterion, also known as the joint maximum-likelihood (JML) criterion. In Section 2.3, we give a brief overview of the maximum-likelihood priority-first search demodulation/decoding algorithm that operates over a tree.

2.1 An OFDM System with Non-Coherent Receiver

Consider an OFDM system with N subchannels, for which the transmission suffers multipath frequency-selective fading. Assume that the fading coefficients $\boldsymbol{h} = \begin{bmatrix} h_\nu \cdots h_1 & h_0 \end{bmatrix}^T$ that are *unknown* to both transmitter and receiver will remain *constant* in a time period T. Denote the information transmitted at time j by

$$\boldsymbol{S}_j = \begin{bmatrix} S_{1,j} \\ S_{2,j} \\ \vdots \\ S_{N,j} \end{bmatrix}_{N \times 1}$$

where each component $S_{i,j}$ is either $\in \{\pm 1\}$ for BPSK or $\in \{\pm 1, \pm \mathsf{i}\}$ for QPSK. The OFDM modulation can be realized by an N-point inverse discrete Fourier transform (DFT), given by

$$\boldsymbol{s}_j = \mathbb{Q}^\dagger \boldsymbol{S}_j = \begin{bmatrix} s_{1,j} \\ s_{2,j} \\ \vdots \\ s_{N,j} \end{bmatrix}_{N\times 1}$$

where

$$\mathbb{Q} = \frac{1}{\sqrt{N}} \begin{bmatrix} e^{-\mathsf{i}\frac{2\pi}{N}(N-1)(N-1)} & \cdots & e^{-\mathsf{i}\frac{2\pi}{N}2(N-1)} & e^{-\mathsf{i}\frac{2\pi}{N}(N-1)} & 1 \\ e^{-\mathsf{i}\frac{2\pi}{N}(N-1)(N-2)} & \cdots & e^{-\mathsf{i}\frac{2\pi}{N}2(N-2)} & e^{-\mathsf{i}\frac{2\pi}{N}(N-2)} & 1 \\ \vdots & \ddots & \vdots & \vdots & \vdots \\ e^{-\mathsf{i}\frac{2\pi}{N}(N-1)} & \cdots & e^{-\mathsf{i}\frac{2\pi}{N}2} & e^{-\mathsf{i}\frac{2\pi}{N}} & 1 \\ 1 & \cdots & 1 & 1 & 1 \end{bmatrix}_{N\times N} \tag{2.1}$$

and superscript "†" denotes the matrix Hermitian transpose operation. The so-called *cyclic prefix* [8] of length ν will then be added before the transmission of $\boldsymbol{s}_j$, resulting in the transmission signal vector as

$$\boldsymbol{p}_j = \begin{bmatrix} p_{1,j} \\ p_{2,j} \\ \vdots \\ p_{L,j} \end{bmatrix} = \begin{bmatrix} s_{1,j} \\ s_{2,j} \\ \vdots \\ s_{N,j} \\ s_{1,j} \\ s_{2,j} \\ \vdots \\ s_{\nu,j} \end{bmatrix}_{L\times 1}$$

where $L = N + \nu$. Here, we assume that $p_{L,j} = s_{\nu,j}$ will be transmitted first, and $p_{1,j} = s_{1,j}$ will be the last one to be sent.

Together with the additive noise $\boldsymbol{v}_j = \left[v_{1,j}, v_{2,j}, \cdots, v_{L,j}\right]^{\mathtt{T}}$, we can formulate the aforementioned system by

$$
\boldsymbol{y}_j = \begin{bmatrix} y_{1,j} \\ y_{2,j} \\ \vdots \\ y_{L,j} \end{bmatrix} = \begin{bmatrix} h_0 & h_1 & h_2 & \cdots & h_{\nu-1} & h_\nu & 0 & \cdots & 0 \\ 0 & h_0 & h_1 & \cdots & h_{\nu-2} & h_{\nu-1} & h_\nu & \cdots & 0 \\ \vdots & \vdots & \vdots & \ddots & \vdots & \vdots & \vdots & \cdots & \vdots \\ 0 & 0 & 0 & \cdots & 0 & h_0 & h_1 & \cdots & h_\nu \\ 0 & 0 & 0 & \cdots & 0 & 0 & h_0 & \cdots & h_{\nu-1} \\ \vdots & \vdots & \vdots & \ddots & \vdots & \vdots & \vdots & \cdots & \vdots \\ 0 & 0 & 0 & \cdots & 0 & 0 & 0 & \cdots & h_0 \end{bmatrix} \begin{bmatrix} p_{1,j} \\ p_{2,j} \\ \vdots \\ p_{L,j} \end{bmatrix} + \begin{bmatrix} v_{1,j} \\ v_{2,j} \\ \vdots \\ v_{L,j} \end{bmatrix}
$$

where $\boldsymbol{v}_j$ is a zero-mean Gaussian noise vector with independent and identically distributed (i.i.d.) entities of covariance matrix $\sigma^2\mathbb{I}_L$, and $\mathbb{I}_L$ is the $L \times L$ identity matrix.

Upon reception of $\boldsymbol{y}_j$, the cyclic prefix will be removed first, which gives a received vector of length N, denoted by $\boldsymbol{x}_j$, i.e.,

$$
\begin{aligned}
\boldsymbol{x}_j &= \begin{bmatrix} x_{1,j} \\ x_{2,j} \\ \vdots \\ x_{N,j} \end{bmatrix} = \begin{bmatrix} y_{1,j} \\ y_{2,j} \\ \vdots \\ y_{N,j} \end{bmatrix} \\
&= \begin{bmatrix} h_0 & h_1 & h_2 & \cdots & h_{\nu-1} & h_\nu & 0 & \cdots & 0 \\ 0 & h_0 & h_1 & \cdots & h_{\nu-2} & h_{\nu-1} & h_\nu & \cdots & 0 \\ \vdots & \vdots & \vdots & \ddots & \vdots & \vdots & \vdots & \cdots & \vdots \\ 0 & 0 & 0 & \cdots & 0 & h_0 & h_1 & \cdots & h_\nu \\ h_\nu & 0 & 0 & \cdots & 0 & 0 & h_0 & \cdots & h_{\nu-1} \\ \vdots & \vdots & \vdots & \ddots & \vdots & \vdots & \vdots & \cdots & \vdots \\ h_1 & h_2 & h_3 & \cdots & h_\nu & 0 & 0 & \cdots & h_0 \end{bmatrix} \boldsymbol{s}_j + \boldsymbol{w}_j \\
&= \mathbb{H}\boldsymbol{s}_j + \boldsymbol{w}_j
\end{aligned}
$$

where

$$
\boldsymbol{w}_j = \begin{bmatrix} w_{1,j} \\ w_{2,j} \\ \vdots \\ w_{N,j} \end{bmatrix} = \begin{bmatrix} v_{1,j} \\ v_{2,j} \\ \vdots \\ v_{N,j} \end{bmatrix}.
$$

Notably, by the circulant property of $\mathbb{H}$, it can be decomposed to $\mathbb{Q}^\dagger\boldsymbol{\Lambda}\mathbb{Q}$ for some diagonal matrix $\boldsymbol{\Lambda}$; hence,

$$
\boldsymbol{x}_j = \mathbb{Q}^\dagger\boldsymbol{\Lambda}\mathbb{Q}\boldsymbol{s}_j + \boldsymbol{w}_j.
$$

The N-point DFT will then be applied onto $\boldsymbol{x}_j$ to obtain

$$\boldsymbol{X}_j = \mathbb{Q}\,\boldsymbol{x}_j = \mathbb{Q}\,\mathbb{Q}^{\dagger}\boldsymbol{\Lambda}\mathbb{Q}\,\boldsymbol{s}_j + \mathbb{Q}\,\boldsymbol{w}_j = \boldsymbol{\Lambda}\boldsymbol{S}_j + \boldsymbol{W}_j$$

where $\boldsymbol{W}_j = \mathbb{Q}\,\boldsymbol{w}_j$. This results in the final formation of the considered system:

$$\boldsymbol{X}_j = \mathbb{S}_j\boldsymbol{\lambda} + \boldsymbol{W}_j. \tag{2.2}$$

In (2.2), we transform vector $\boldsymbol{S}_j$ to its equivalent diagonal matrix $\mathbb{S}_j$ as

$$\mathbb{S}_j = \begin{bmatrix} S_{1,j} & 0 & \cdots & 0 \\ 0 & S_{2,j} & \cdots & 0 \\ \vdots & \vdots & \ddots & \vdots \\ 0 & 0 & \cdots & S_{N,j} \end{bmatrix}_{N\times N}$$

and the elements of vector $\boldsymbol{\lambda} = \begin{bmatrix}\lambda_{N-1} & \cdots & \lambda_1 & \lambda_0\end{bmatrix}^{\mathrm{T}}$ are the DFT values of the channel fading $\boldsymbol{h}$, given by

$$\boldsymbol{\Lambda} = \begin{bmatrix} \lambda_{N-1} & 0 & \cdots & 0 \\ 0 & \lambda_{N-2} & \cdots & 0 \\ \vdots & \vdots & \ddots & \vdots \\ 0 & 0 & \cdots & \lambda_0 \end{bmatrix} = \mathbb{Q} \begin{bmatrix} h_0 & h_1 & h_2 & \cdots & h_{\nu-1} & h_\nu & 0 & \cdots & 0 \\ 0 & h_0 & h_1 & \cdots & h_{\nu-2} & h_{\nu-1} & h_\nu & \cdots & 0 \\ \vdots & \vdots & \vdots & \ddots & \vdots & \vdots & \vdots & \cdots & \vdots \\ 0 & 0 & 0 & \cdots & 0 & h_0 & h_1 & \cdots & h_\nu \\ h_\nu & 0 & 0 & \cdots & 0 & 0 & h_0 & \cdots & h_{\nu-1} \\ \vdots & \vdots & \vdots & \ddots & \vdots & \vdots & \vdots & \cdots & \vdots \\ h_1 & h_2 & h_3 & \cdots & h_\nu & 0 & 0 & \cdots & h_0 \end{bmatrix} \mathbb{Q}^{\dagger}.$$

After introducing the basic model of an OFDM system, we next turn to the non-coherent detection of OFDM symbols. It can be verified that it requires at least two OFDM symbols to perform non-coherent detection at the receiver; hence, we assume that $T \geq 2T_s$, where as having been defined previously, T is the period that channel coefficients $\boldsymbol{h}$ remain constant, and T_s is the OFDM symbol duration. Without loss of generality, let the two OFDM symbols received are indexed by 1 and 2. This gives

$$\boldsymbol{X}_1 = \mathbb{S}_1\boldsymbol{\lambda} + \boldsymbol{W}_1 \tag{2.3}$$

and

$$\boldsymbol{X}_2 = \mathbb{S}_2\boldsymbol{\lambda} + \boldsymbol{W}_2 \tag{2.4}$$

For convenience, we will combine (2.3) and (2.4) into

$$\vec{\boldsymbol{X}} = \vec{\boldsymbol{S}}\boldsymbol{\lambda} + \vec{\boldsymbol{W}} \tag{2.5}$$

where

$$\vec{\boldsymbol{X}} = \begin{bmatrix}\boldsymbol{X}_1\\ \boldsymbol{X}_2\end{bmatrix}, \quad \vec{\boldsymbol{S}} = \begin{bmatrix}\mathbb{S}_1\\ \mathbb{S}_2\end{bmatrix} \quad \text{and} \quad \vec{\boldsymbol{W}} = \begin{bmatrix}\boldsymbol{W}_1\\ \boldsymbol{W}_2\end{bmatrix}.$$

Notably, if $T \geq kT_s$, we can of course consider a non-coherent receiver for the information $\vec{\boldsymbol{S}} = \left[\mathbb{S}_1, \mathbb{S}_2, \ldots, \mathbb{S}_k\right]^T$. However, since the demodulation complexity dramatically grows as k increases and since a larger k implies the resulting system can be only used in a less mobile environment, this thesis only considers the case of $k = 2$.

2.2 General Likelihood Ratio Test (GLRT) Criterion

Equation (2.5) defines the system model considered in this thesis. Two assumptions are then made for this system: (i) both transmitter and receiver knows the memory order of the channel ν, but (ii) none of them has the knowledge about channel fading $\boldsymbol{\lambda}$. With the assumptions above, it can be derived that the least square estimate of the channel coefficient $\boldsymbol{\lambda}$ for a given $\vec{\boldsymbol{S}}$ is equal to $\hat{\boldsymbol{\lambda}} = (\vec{\boldsymbol{S}}^\dagger \vec{\boldsymbol{S}})^{-1}\vec{\boldsymbol{S}}^\dagger \vec{\boldsymbol{X}}$, if the $\boldsymbol{\lambda}$ considered in the below minimization lie in the N-dimensional complex space $\mathcal{C}^N$. Thus, the so-called general likelihood ratio test (GLRT) decision [8] can be written as

$$\hat{\vec{\boldsymbol{S}}} = \arg\min_{\vec{\boldsymbol{S}}\in\mathcal{S}}\min_{\boldsymbol{\lambda}\in\mathcal{C}^N}\|\vec{\boldsymbol{X}} - \vec{\boldsymbol{S}}\boldsymbol{\lambda}\|^2 = \arg\min_{\vec{\boldsymbol{S}}\in\mathcal{S}}\|\vec{\boldsymbol{X}} - \vec{\boldsymbol{S}}\hat{\boldsymbol{\lambda}}\|^2 = \arg\min_{\vec{\boldsymbol{S}}\in\mathcal{S}}\|\vec{\boldsymbol{X}} - \mathbb{P}_{\vec{\boldsymbol{S}}}\vec{\boldsymbol{X}}\|^2 \tag{2.6}$$

where

$$
\begin{aligned}
\mathbb{P}_{\vec{\boldsymbol{S}}} &\triangleq \vec{\boldsymbol{S}}(\vec{\boldsymbol{S}}^{\dagger}\vec{\boldsymbol{S}})^{-1}\vec{\boldsymbol{S}}^{\dagger} \\
&= \vec{\boldsymbol{S}} \begin{bmatrix} \frac{1}{|S_{1,1}|^2+|S_{1,2}|^2} & 0 & \cdots & 0 \\ 0 & \frac{1}{|S_{2,1}|^2+|S_{2,2}|^2} & \cdots & 0 \\ \vdots & \vdots & \ddots & \vdots \\ 0 & 0 & \cdots & \frac{1}{|S_{N,1}|^2+|S_{N,2}|^2} \end{bmatrix} \vec{\boldsymbol{S}}^{\dagger} \\
&= \begin{bmatrix}
\frac{|S_{1,1}|^2}{|S_{1,1}|^2+|S_{1,2}|^2} & 0 & \cdots & 0 & \frac{S_{1,1}S_{1,2}^*}{|S_{1,1}|^2+|S_{1,2}|^2} & 0 & \cdots & 0 \\
0 & \frac{|S_{2,1}|^2}{|S_{2,1}|^2+|S_{2,2}|^2} & \cdots & 0 & 0 & \frac{S_{2,1}S_{2,2}^*}{|S_{2,1}|^2+|S_{2,2}|^2} & \cdots & 0 \\
\vdots & \vdots & \ddots & \vdots & \vdots & \vdots & \ddots & \vdots \\
0 & 0 & \cdots & \frac{|S_{N,1}|^2}{|S_{N,1}|^2+|S_{N,2}|^2} & 0 & 0 & \cdots & \frac{S_{N,1}S_{N,2}^*}{|S_{N,1}|^2+|S_{N,2}|^2} \\
\frac{S_{1,1}^*S_{1,2}}{|S_{1,1}|^2+|S_{1,2}|^2} & 0 & \cdots & 0 & \frac{|S_{1,2}|^2}{|S_{1,1}|^2+|S_{1,2}|^2} & 0 & \cdots & 0 \\
0 & \frac{S_{2,1}^*S_{2,2}}{|S_{2,1}|^2+|S_{2,2}|^2} & \cdots & 0 & 0 & \frac{|S_{2,2}|^2}{|S_{2,1}|^2+|S_{2,2}|^2} & \cdots & 0 \\
\vdots & \vdots & \ddots & \vdots & \vdots & \vdots & \ddots & \vdots \\
0 & 0 & \cdots & \frac{S_{N,1}^*S_{N,2}}{|S_{N,1}|^2+|S_{N,2}|^2} & 0 & 0 & \cdots & \frac{|S_{N,2}|^2}{|S_{N,1}|^2+|S_{N,2}|^2}
\end{bmatrix}.
\end{aligned}
$$

We can further derive that

$$
\begin{aligned}
\hat{\vec{\boldsymbol{S}}} &= \arg\min_{\vec{\boldsymbol{S}}\in\mathcal{S}} \|\vec{\boldsymbol{X}} - \mathbb{P}_{\vec{\boldsymbol{S}}}\vec{\boldsymbol{X}}\|^2 \\
&= \arg\max_{\vec{\boldsymbol{S}}\in\mathcal{S}} \vec{\boldsymbol{X}}^{\dagger}\mathbb{P}_{\vec{\boldsymbol{S}}}\vec{\boldsymbol{X}} \\
&= \arg\max_{\vec{\boldsymbol{S}}\in\mathcal{S}} \sum_{i=1}^{N} \frac{|X_{i,1}|^2|S_{i,1}|^2 + |X_{i,2}|^2|S_{i,2}|^2 + X_{i,1}S_{i,1}^*X_{i,2}^*S_{i,2} + X_{i,1}^*S_{i,1}X_{i,2}S_{i,2}^*}{|S_{i,1}|^2+|S_{i,2}|^2} \\
&= \arg\max_{\vec{\boldsymbol{S}}\in\mathcal{S}} \sum_{i=1}^{N} \frac{|S_{i,1}X_{i,1}^* + S_{i,2}X_{i,2}^*|^2}{|S_{i,1}|^2+|S_{i,2}|^2} \qquad (2.7)
\end{aligned}
$$

As a consequence of (2.7), $(S_{i,1}, S_{i,2}) = (1, -1)$ and $(S_{i,1}, S_{i,2}) = (-1, 1)$ (similarly, $(S_{i,1}, S_{i,2}) = (1, 1)$ and $(S_{i,1}, S_{i,2}) = (-1, -1)$) are indistinguishable at the receiver; hence, one of $S_{i,1}$ and $S_{i,2}$ must be fixed (say, as -1) for BPSK. The same reason gives that one of $S_{i,1}$ and $S_{i,2}$ must be fixed (say, as $\frac{1}{\sqrt{2}} - \frac{\mathrm{i}}{\sqrt{2}}$) also for QPSK. As an example, a GLRT-detectable transmission signal can be assigned as

$$\vec{\boldsymbol{S}} = \begin{bmatrix} \boldsymbol{S}_1 \\ \boldsymbol{S}_2 \end{bmatrix} = \begin{bmatrix} -1 & 0 & 0 & \cdots & 0 \\ 0 & S_{2,1} & 0 & \cdots & 0 \\ 0 & 0 & S_{3,1} & \cdots & 0 \\ \vdots & \vdots & \vdots & \ddots & \vdots \\ 0 & 0 & 0 & \cdots & -1 \\ S_{1,2} & 0 & 0 & \cdots & 0 \\ 0 & -1 & 0 & \cdots & 0 \\ 0 & 0 & -1 & \cdots & 0 \\ \vdots & \vdots & \vdots & \ddots & \vdots \\ 0 & 0 & 0 & \cdots & S_{N,2} \end{bmatrix}. \tag{2.8}$$

2.3 Maximum-Likelihood Priority-First Search Decoding Algorithm

One effective structure for demodulating $\vec{\boldsymbol{S}}$ is to represent all possible transmission signals by a tree. As an example for BPSK, each branch on a tree is labelled by two information bits $S_{i,1}S_{i,2}$ as shown in Figure 2.1. Each node have only two (respectively, four) branches emitting from it for the case of BPSK (respectively, QPSK) because one of $S_{i,1}$ and $S_{i,2}$ must be fixed. In this figure, we circle these fixed bits so that they can be more clearly seen. We denote the path ending at level ℓ by the labels it has traversed, i.e., $\vec{\boldsymbol{S}}_{(\ell)} = [S_{1,1}S_{1,2}S_{2,1}S_{2,2}\cdots S_{\ell,1}S_{\ell,2}]^{\mathtt{T}}$. Here with no ambiguity, we abuse the notation by re-using $\vec{\boldsymbol{S}}_{(\ell)}$, which originally denotes the information signal matrix, to denote the equivalent vector. For notational convenience, we will drop the subscript in notation $\vec{\boldsymbol{S}}_{(\ell)}$ when $\ell = N$.

The *priority-first search algorithm* is a kind of graph search algorithm. It searches the graph by expanding the most promising path. It can then be used onto the tree we constructed for information signal $\vec{\boldsymbol{S}}$.

A typical priority-first search algorithm is given below [3]:

Step 1. Load the stack with the path that ends at the original node at level 0.

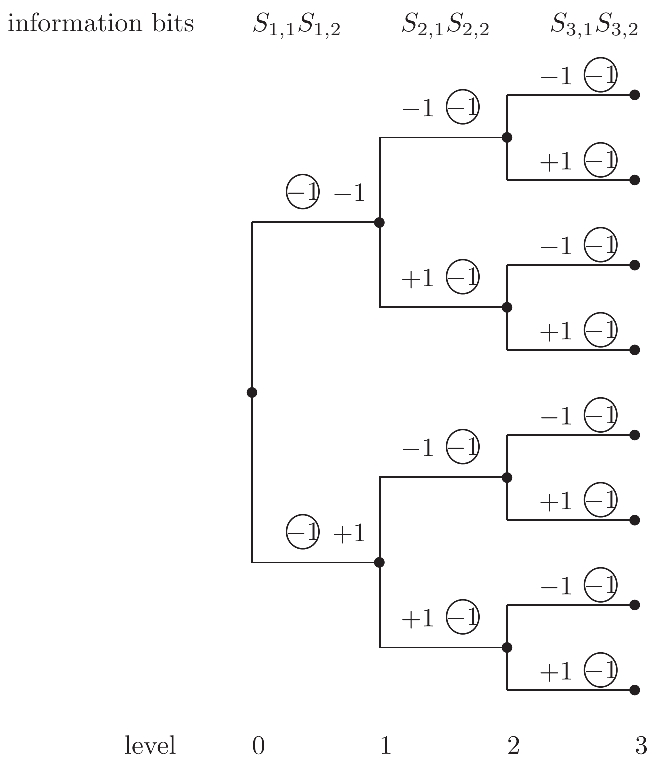

Figure 2.1: Illustration of a tree structure, up to level 3, corresponding to information signal in (2.8) with fixed bits circled.

Step 2. Insert the successor paths of the current top path into the stack such that the paths in the stack are ordered according to their ascending metric values f; then, delete this top path from the stack.

Step 3. If the new top path in the stack ends at a terminal node in the tree at level N, output the labels corresponding to the top path, and stop the algorithm; otherwise, go to Step 2.

Next we quote a sufficient condition from [3], under which the priority-first search algorithm guarantees to expand the path (cf. Step 2), whose metric is the smallest among all paths of the same length.

Lemma 2.1 *If the metric f is nondecreasing along every path in the tree, i.e.,*

$$f(\vec{\boldsymbol{S}}_{(\ell)}) \leq \min_{\{\tilde{\vec{\boldsymbol{S}}} \in \mathcal{S}: \tilde{\vec{\boldsymbol{S}}}_{(\ell)} = \vec{\boldsymbol{S}}_{(\ell)}\}} f(\tilde{\vec{\boldsymbol{S}}}) \tag{2.9}$$

then the priority-first search algorithm always yields the path with the smallest metric value among all paths of the same length.

Usually, a metric f is defined as the sum of two parts:

$$f(\vec{\boldsymbol{S}}_{(\ell)}) \triangleq g(\vec{\boldsymbol{S}}_{(\ell)}) + \varphi(\vec{\boldsymbol{S}}_{(\ell)}).$$

The former part g is determined based on the maximum-likelihood metric and hence satisfies

$$\arg\min_{\vec{\boldsymbol{S}} \in \mathcal{S}} g(\vec{\boldsymbol{S}}) = \arg\min_{\vec{\boldsymbol{S}} \in \mathcal{S}} \|\vec{\boldsymbol{X}} - \mathbb{P}_{\vec{\boldsymbol{S}}} \vec{\boldsymbol{X}}\|^2.$$

The latter part φ is often named *heuristic function*. It gives the prediction of the route from the current node to an end node at level N so as to speed up the search process. Note that the heuristic function is not unique, and different designs will lead to distinct computational complexities.

Chapter 3

Modified GLRT and Priority First Search Demodulator

In this chapter, we will focus on the derivation of the modified GLRT that we propose in this thesis. The maximum-likelihood metrics respectively for the GLRT and the modified GLRT for use of the priority-first search demodulator will be subsequently derived.

3.1 The Modified GLRT

In Section 2.1, the channel coefficient matrix $\mathbb{H}$ can be decomposed into $\mathbb{Q}^\dagger \boldsymbol{\Lambda} \mathbb{Q}$. Equivalently, we can write $\boldsymbol{\Lambda} = \mathbb{Q}\mathbb{H}\mathbb{Q}^\dagger$. The GLRT then demodulates the transmitted signal through (2.6), i.e.,

$$\hat{\vec{\boldsymbol{S}}} = \arg\min_{\vec{\boldsymbol{S}} \in \mathcal{S}} \min_{\boldsymbol{\lambda} \in \mathcal{C}^N} \|\vec{\boldsymbol{X}} - \vec{\boldsymbol{S}}\boldsymbol{\lambda}\|^2. \tag{3.1}$$

The range of minimization in (3.1) is the entire N-dimensional complex domain $\mathcal{C}^N$. We however observe that the possible values of $\boldsymbol{\lambda}$ should be much smaller than this N-dimensional complex domain. Take $N = 3$ and $\nu = 1$ as an example. We obtain from (2.1) that

$$\begin{aligned} \mathbb{Q} &= \frac{1}{\sqrt{3}} \begin{bmatrix} -\frac{1}{2} - \mathsf{i}\frac{\sqrt{3}}{2} & -\frac{1}{2} + \mathsf{i}\frac{\sqrt{3}}{2} & 1 \\ -\frac{1}{2} + \mathsf{i}\frac{\sqrt{3}}{2} & -\frac{1}{2} - \mathsf{i}\frac{\sqrt{3}}{2} & 1 \\ 1 & 1 & 1 \end{bmatrix} \\ &= \frac{1}{\sqrt{3}} \begin{bmatrix} \boldsymbol{q}_1 & \boldsymbol{q}_2 & \boldsymbol{q}_3 \end{bmatrix}. \end{aligned}$$

Also note that

$$\mathbb{H} = \begin{bmatrix} h_0 & h_1 & 0 \\ 0 & h_0 & h_1 \\ h_1 & 0 & h_0 \end{bmatrix}.$$

Hence,

$$\boldsymbol{\Lambda} = \mathbb{Q}\mathbb{H}\mathbb{Q}^\dagger = \begin{bmatrix} \lambda_2 & 0 & 0 \\ 0 & \lambda_1 & 0 \\ 0 & 0 & \lambda_0 \end{bmatrix} = \begin{bmatrix} h_0 + h_1\left(-\frac{1}{2} + \mathsf{i}\frac{\sqrt{3}}{2}\right) & 0 & 0 \\ 0 & h_0 + h_1\left(-\frac{1}{2} - \mathsf{i}\frac{\sqrt{3}}{2}\right) & 0 \\ 0 & 0 & h_0 + h_1 \end{bmatrix}$$

or equivalently,

$$\boldsymbol{\lambda} = \begin{bmatrix} \lambda_2 \\ \lambda_1 \\ \lambda_0 \end{bmatrix} = (h_0\boldsymbol{q}_3 + h_1\boldsymbol{q}_2) = \begin{bmatrix} \boldsymbol{q}_2 & \boldsymbol{q}_3 \end{bmatrix} \begin{bmatrix} h_1 \\ h_0 \end{bmatrix} = \mathbb{Q}_1\boldsymbol{h}.$$

Therefore, $\boldsymbol{\lambda}$ should lie only in a 2-dimensional plane over the 3-dimensional complex space.

By following the same derivation, it can be derived for general N and $\nu < N$ that

$$\boldsymbol{\lambda} = \mathbb{Q}_\nu \boldsymbol{h} \tag{3.2}$$

where

$$\mathbb{Q}_\nu = \begin{bmatrix} \boldsymbol{q}_{N-\nu} \cdots \boldsymbol{q}_N \end{bmatrix}.$$

Thus, the non-coherent GLRT demodulator/decoder can be written as

$$\hat{\vec{\boldsymbol{S}}} = \arg\min_{\vec{\boldsymbol{S}}\in\mathcal{S}} \min_{\boldsymbol{h}\in\mathcal{C}^{\nu+1}} \|\vec{\boldsymbol{X}} - \vec{\boldsymbol{S}}\mathbb{Q}_\nu\boldsymbol{h}\|^2$$

With the two assumptions in Section 2.2, the least square estimate of channel fading $\boldsymbol{h}$ for given $\vec{\boldsymbol{S}}$ is equal to $\hat{\boldsymbol{h}} = (\tilde{\boldsymbol{S}}^\dagger\tilde{\boldsymbol{S}})^{-1}\tilde{\boldsymbol{S}}^\dagger\vec{\boldsymbol{X}}$; here $\tilde{\boldsymbol{S}} \triangleq \vec{\boldsymbol{S}}\mathbb{Q}_\nu$. Therefore, the modified version of general likelihood ratio test (i.e., the modified GLRT) decision can be written as

$$\hat{\vec{\boldsymbol{S}}} = \arg\min_{\vec{\boldsymbol{S}}\in\mathcal{S}} \|\vec{\boldsymbol{X}} - \vec{\boldsymbol{S}}\mathbb{Q}_\nu\hat{\boldsymbol{h}}\|^2 = \arg\min_{\vec{\boldsymbol{S}}\in\mathcal{S}} \|\vec{\boldsymbol{X}} - \mathbb{P}_{\tilde{\boldsymbol{S}}}\vec{\boldsymbol{X}}\|^2 \tag{3.3}$$

where $\mathbb{P}_{\tilde{\boldsymbol{S}}} = \tilde{\boldsymbol{S}}(\tilde{\boldsymbol{S}}^\dagger \tilde{\boldsymbol{S}})^{-1}\tilde{\boldsymbol{S}}^\dagger$. In comparison with the estimate of $\boldsymbol{\lambda}$ without any limitation (i.e., the GLRT), the resulting $\boldsymbol{\lambda}$ corresponding to the new estimate of $\boldsymbol{h}$ now lies in a $(\nu+1)$-dimensional hyperplane, defined via $\boldsymbol{\lambda} = \mathbb{Q}_\nu \boldsymbol{h}$. By using the modified GLRT instead of the GLRT, we expect that the probability of error will decrease as the latter may give an $\boldsymbol{\lambda}$ estimate that cannot be obtained by the real channel.

We can further derive that

$$\begin{aligned}
\hat{\vec{\boldsymbol{S}}} &= \arg\min_{\vec{\boldsymbol{S}}\in\mathcal{S}} \|\vec{\boldsymbol{X}} - \mathbb{P}_{\tilde{\boldsymbol{S}}}\vec{\boldsymbol{X}}\|^2 \\
&= \arg\min_{\vec{\boldsymbol{S}}\in\mathcal{S}} (\vec{\boldsymbol{X}} - \mathbb{P}_{\tilde{\boldsymbol{S}}}\vec{\boldsymbol{X}})^\dagger(\vec{\boldsymbol{X}} - \mathbb{P}_{\tilde{\boldsymbol{S}}}\vec{\boldsymbol{X}}) \\
&= \arg\min_{\vec{\boldsymbol{S}}\in\mathcal{S}} \Big(\|\vec{\boldsymbol{X}}\|^2 - \vec{\boldsymbol{X}}^\dagger \mathbb{P}_{\tilde{\boldsymbol{S}}}\vec{\boldsymbol{X}} - \vec{\boldsymbol{X}}^\dagger \mathbb{P}^\dagger_{\tilde{\boldsymbol{S}}}\vec{\boldsymbol{X}} + \vec{\boldsymbol{X}}^\dagger \mathbb{P}^\dagger_{\tilde{\boldsymbol{S}}}\mathbb{P}_{\tilde{\boldsymbol{S}}}\vec{\boldsymbol{X}}\Big)
\end{aligned}$$

It is apparent that $\|\vec{\boldsymbol{X}}\|^2$ can be removed as it is nothing to do with the optimizer. Also, by

$$(\tilde{\boldsymbol{S}}^\dagger \tilde{\boldsymbol{S}})^{-1} = \Big(\mathbb{Q}_\nu^\dagger \vec{\boldsymbol{S}}^\dagger \vec{\boldsymbol{S}} \mathbb{Q}_\nu\Big)^{-1} = \big(\mathbb{Q}_\nu^\dagger 2\mathbb{I}_N \mathbb{Q}_\nu\big)^{-1} = \frac{1}{2}\mathbb{I}_{\nu+1},$$

we have

$$\begin{aligned}
\mathbb{P}_{\tilde{\boldsymbol{S}}} &= \tilde{\boldsymbol{S}}(\tilde{\boldsymbol{S}}^\dagger \tilde{\boldsymbol{S}})^{-1}\tilde{\boldsymbol{S}}^\dagger \\
&= \frac{1}{2} \times \tilde{\boldsymbol{S}}\tilde{\boldsymbol{S}}^\dagger \\
&= \frac{1}{2} \times \vec{\boldsymbol{S}}\mathbb{Q}_\nu \mathbb{Q}_\nu^\dagger \vec{\boldsymbol{S}}^\dagger,
\end{aligned}$$

which implies

$$\mathbb{P}_{\tilde{\boldsymbol{S}}} = \mathbb{P}^\dagger_{\tilde{\boldsymbol{S}}} = \mathbb{P}^\dagger_{\tilde{\boldsymbol{S}}}\mathbb{P}_{\tilde{\boldsymbol{S}}}.$$

So

$$\begin{aligned}
\hat{\vec{\boldsymbol{S}}} &= \arg\min_{\vec{\boldsymbol{S}}\in\mathcal{S}} \big(-\vec{\boldsymbol{X}}^\dagger \mathbb{P}_{\tilde{\boldsymbol{S}}}\vec{\boldsymbol{X}}\big) \\
&= \arg\max_{\vec{\boldsymbol{S}}\in\mathcal{S}} \vec{\boldsymbol{X}}^\dagger \mathbb{P}_{\tilde{\boldsymbol{S}}}\vec{\boldsymbol{X}} \\
&= \arg\max_{\vec{\boldsymbol{S}}\in\mathcal{S}} \vec{\boldsymbol{X}}^\dagger \vec{\boldsymbol{S}}\mathbb{Q}_\nu \mathbb{Q}_\nu^\dagger \vec{\boldsymbol{S}}^\dagger \vec{\boldsymbol{X}}. \qquad (3.4)
\end{aligned}$$

(3.4) will be used in later simulations for performance comparisons between the modified GLRT and the GLRT. Again, we take $N = 2$ and $\nu = 1$ as an example for its computation. In such case, we have

$$\vec{\boldsymbol{S}} = \begin{bmatrix} S_{1,1} & 0 \\ 0 & S_{2,1} \\ S_{1,2} & 0 \\ 0 & S_{2,2} \end{bmatrix} \quad \text{and} \quad \vec{\boldsymbol{X}} = \begin{bmatrix} X_{1,1} \\ X_{2,1} \\ X_{1,2} \\ X_{2,2} \end{bmatrix}.$$

For convenience, we denote

$$\mathbb{Q}_\nu \mathbb{Q}_\nu^\dagger = \begin{bmatrix} q_{1,1} & q_{1,2} \\ q_{2,1} & q_{2,2} \end{bmatrix}.$$

Hence,

$$\begin{aligned}
\mathbb{P}_{\tilde{\boldsymbol{S}}} &= \begin{bmatrix} S_{1,1} & 0 \\ 0 & S_{2,1} \\ S_{1,2} & 0 \\ 0 & S_{2,2} \end{bmatrix} \begin{bmatrix} q_{1,1} & q_{1,2} \\ q_{2,1} & q_{2,2} \end{bmatrix} \begin{bmatrix} S_{1,1}^* & 0 & S_{1,2}^* & 0 \\ 0 & S_{2,1}^* & 0 & S_{2,2}^* \end{bmatrix} \\
&= \begin{bmatrix} S_{1,1}q_{1,1} & S_{1,1}q_{1,2} \\ S_{2,1}q_{2,1} & S_{2,1}q_{2,2} \\ S_{1,2}q_{1,1} & S_{1,2}q_{1,2} \\ S_{2,2}q_{2,1} & S_{2,2}q_{2,2} \end{bmatrix} \begin{bmatrix} S_{1,1}^* & 0 & S_{1,2}^* & 0 \\ 0 & S_{2,1}^* & 0 & S_{2,2}^* \end{bmatrix} \\
&= \begin{bmatrix} S_{1,1}^* S_{1,1} q_{1,1} & S_{2,1}^* S_{1,1} q_{1,2} & S_{1,2}^* S_{1,1} q_{1,1} & S_{2,2}^* S_{1,1} q_{1,2} \\ S_{1,1}^* S_{2,1} q_{2,1} & S_{2,1}^* S_{2,1} q_{2,2} & S_{1,2}^* S_{2,1} q_{2,1} & S_{2,2}^* S_{2,1} q_{2,2} \\ S_{1,1}^* S_{1,2} q_{1,1} & S_{2,1}^* S_{1,2} q_{1,2} & S_{1,2}^* S_{1,2} q_{1,1} & S_{2,2}^* S_{1,2} q_{1,2} \\ S_{1,1}^* S_{2,2} q_{2,1} & S_{2,1}^* S_{2,2} q_{2,2} & S_{1,2}^* S_{2,2} q_{2,1} & S_{2,2}^* S_{2,2} q_{2,2} \end{bmatrix}
\end{aligned}$$

where the superscript "*" denotes the complex conjugate operation. Consequently, the demodulator/decoder output with respect to $\vec{\boldsymbol{S}}$ is given by:

$$
\begin{aligned}
\hat{\vec{\boldsymbol{S}}} &= \arg\max_{\vec{\boldsymbol{S}}\in\mathcal{S}} \vec{\boldsymbol{X}}^{\dagger}\mathbb{P}_{\tilde{\boldsymbol{S}}}\vec{\boldsymbol{X}} \\
&= \begin{bmatrix} X_{1,1}^* X_{2,1}^* X_{1,2}^* X_{2,2}^* \end{bmatrix} \begin{bmatrix} S_{1,1}^*S_{1,1}q_{1,1} & S_{2,1}^*S_{1,1}q_{1,2} & S_{1,2}^*S_{1,1}q_{1,1} & S_{2,2}^*S_{1,1}q_{1,2} \\ S_{1,1}^*S_{2,1}q_{2,1} & S_{2,1}^*S_{2,1}q_{2,2} & S_{1,2}^*S_{2,1}q_{2,1} & S_{2,2}^*S_{2,1}q_{2,2} \\ S_{1,1}^*S_{1,2}q_{1,1} & S_{2,1}^*S_{1,2}q_{1,2} & S_{1,2}^*S_{1,2}q_{1,1} & S_{2,2}^*S_{1,2}q_{1,2} \\ S_{1,1}^*S_{2,2}q_{2,1} & S_{2,1}^*S_{2,2}q_{2,2} & S_{1,2}^*S_{2,2}q_{2,1} & S_{2,2}^*S_{2,2}q_{2,2} \end{bmatrix} \begin{bmatrix} X_{1,1} \\ X_{2,1} \\ X_{1,2} \\ X_{2,2} \end{bmatrix} \\
&= \begin{bmatrix} X_{1,1}^* X_{2,1}^* X_{1,2}^* X_{2,2}^* \end{bmatrix} \begin{bmatrix} X_{1,1}S_{1,1}^*S_{1,1}q_{1,1} + X_{2,1}S_{2,1}^*S_{1,1}q_{1,2} + X_{1,2}S_{1,2}^*S_{1,1}q_{1,1} + X_{2,2}S_{2,2}^*S_{1,1}q_{1,2} \\ X_{1,1}S_{1,1}^*S_{2,1}q_{2,1} + X_{2,1}S_{2,1}^*S_{2,1}q_{2,2} + X_{1,2}S_{1,2}^*S_{2,1}q_{2,1} + X_{2,2}S_{2,2}^*S_{2,1}q_{2,2} \\ X_{1,1}S_{1,1}^*S_{1,2}q_{1,1} + X_{2,1}S_{2,1}^*S_{1,2}q_{1,2} + X_{1,2}S_{1,2}^*S_{1,2}q_{1,1} + X_{2,2}S_{2,2}^*S_{1,2}q_{1,2} \\ X_{1,1}S_{1,1}^*S_{2,2}q_{2,1} + X_{2,1}S_{2,1}^*S_{2,2}q_{2,2} + X_{1,2}S_{1,2}^*S_{2,2}q_{2,1} + X_{2,2}S_{2,2}^*S_{2,2}q_{2,2} \end{bmatrix} \\
&= X_{1,1}^*X_{1,1}S_{1,1}^*S_{1,1}q_{1,1} + X_{1,1}^*X_{2,1}S_{2,1}^*S_{1,1}q_{1,2} + X_{1,1}^*X_{1,2}S_{1,2}^*S_{1,1}q_{1,1} + X_{1,1}^*X_{2,2}S_{2,2}^*S_{1,1}q_{1,2} \\
&+ X_{2,1}^*X_{1,1}S_{1,1}^*S_{2,1}q_{2,1} + X_{2,1}^*X_{2,1}S_{2,1}^*S_{2,1}q_{2,2} + X_{2,1}^*X_{1,2}S_{1,2}^*S_{2,1}q_{2,1} + X_{2,1}^*X_{2,2}S_{2,2}^*S_{2,1}q_{2,2} \\
&+ X_{1,2}^*X_{1,1}S_{1,1}^*S_{1,2}q_{1,1} + X_{1,2}^*X_{2,1}S_{2,1}^*S_{1,2}q_{1,2} + X_{1,2}^*X_{1,2}S_{1,2}^*S_{1,2}q_{1,1} + X_{1,2}^*X_{2,2}S_{2,2}^*S_{1,2}q_{1,2} \\
&+ X_{2,2}^*X_{1,1}S_{1,1}^*S_{2,2}q_{2,1} + X_{2,2}^*X_{2,1}S_{2,1}^*S_{2,2}q_{2,2} + X_{2,2}^*X_{1,2}S_{1,2}^*S_{2,2}q_{2,1} + X_{2,2}^*X_{2,2}S_{2,2}^*S_{2,2}q_{2,2}
\end{aligned}
$$

It is obvious from the above expression that $\vec{\boldsymbol{X}}^{\dagger}\mathbb{P}_{\tilde{\boldsymbol{S}}}\vec{\boldsymbol{X}} = \vec{\boldsymbol{X}}^{\dagger}\mathbb{P}_{-\tilde{\boldsymbol{S}}}\vec{\boldsymbol{X}}$. In other words, the following two OFDM symbols are indistinguishable at the receiver.

$$
\vec{\boldsymbol{S}} = \begin{bmatrix} -1 & 0 \\ 0 & -1 \\ +1 & 0 \\ 0 & -1 \end{bmatrix} \quad \text{and} \quad -\vec{\boldsymbol{S}} = \begin{bmatrix} +1 & 0 \\ 0 & +1 \\ -1 & 0 \\ 0 & +1 \end{bmatrix}.
$$

Therefore, we should fix at least one component of an OFDM symbol $\vec{\boldsymbol{S}}$. For instance, we can fix $S_{1,1} = -1$ for BPSK or $S_{1,1} = \frac{1}{\sqrt{2}} - \frac{\mathrm{i}}{\sqrt{2}}$ for QPSK. This is contrary to the GLRT (cf. (2.8)), where half of the OFDM components should be fixed. Note that although the modified GLRT can reach a much higher data rate by fixing only one component in an OFDM symbol, we will in later simulations fix half of the components in order to compare the performance of the modified GLRT with that of the GLRT under the same data rate.

We close this subsection by a simple lemma about the equivalence of the modified GLRT and the GLRT.

Lemma 3.1 *When $\nu = N-1$, (3.4) is reduced to the GLRT.*

Proof: When $\nu = N-1$, we immediately have

$$\mathbb{Q}_\nu = \left[\boldsymbol{q}_1 \boldsymbol{q}_2 \cdots \boldsymbol{q}_N\right] = \sqrt{N}\mathbb{Q}$$

and

$$\tilde{\boldsymbol{S}} = \vec{\boldsymbol{S}}\mathbb{Q}_\nu = \vec{\boldsymbol{S}}\sqrt{N}\mathbb{Q}.$$

The resulting $\mathbb{P}_{\tilde{\boldsymbol{S}}}$ is therefore equal to

$$\begin{aligned}
\mathbb{P}_{\tilde{\boldsymbol{S}}} &= \tilde{\boldsymbol{S}}(\tilde{\boldsymbol{S}}^\dagger \tilde{\boldsymbol{S}})^{-1}\tilde{\boldsymbol{S}}^\dagger \\
&= (\vec{\boldsymbol{S}}\sqrt{N}\mathbb{Q})\left((\vec{\boldsymbol{S}}\sqrt{N}\mathbb{Q})^\dagger(\vec{\boldsymbol{S}}\sqrt{N}\mathbb{Q})\right)^{-1}(\vec{\boldsymbol{S}}\sqrt{N}\mathbb{Q})^\dagger \\
&= (\vec{\boldsymbol{S}}\mathbb{Q})(\mathbb{Q}^\dagger\vec{\boldsymbol{S}}^\dagger\vec{\boldsymbol{S}}\mathbb{Q})^{-1}(\vec{\boldsymbol{S}}\mathbb{Q})^\dagger \\
&= \vec{\boldsymbol{S}}\mathbb{Q}\mathbb{Q}^{-1}(\vec{\boldsymbol{S}}^\dagger\vec{\boldsymbol{S}})^{-1}(\mathbb{Q}^\dagger)^{-1}\mathbb{Q}^\dagger\vec{\boldsymbol{S}}^\dagger \\
&= \vec{\boldsymbol{S}}(\vec{\boldsymbol{S}}^\dagger\vec{\boldsymbol{S}})^{-1}\vec{\boldsymbol{S}}^\dagger \\
&= \mathbb{P}_{\vec{\boldsymbol{S}}}.
\end{aligned}$$

Hence, (3.4) is reduced to the GLRT. □

By this lemma, we conclude that the modified GLRT decision is equivalent to the GLRT decision when $\nu = N-1$. In such case, the range of minimization with respect to $\boldsymbol{h}$ for the modified GLRT and that of the $\boldsymbol{\lambda}$ for the GLRT are both the N-dimensional complex space $\mathcal{C}^N$.

3.2 The Maximum-Likelihood Demodulation Metric for the Modified GLRT

In this section, we will derive the recursive metric formulas that are used by the priority-first search algorithm under the modified GLRT criterion. Two formulas will be provided:

The first metric f_1 allows the demodulation to be performed by sequentially feeding the components of an OFDM symbol, while the second one f_2 requires parallelly using all components of an OFDM symbol at each recursion step. Both recursive metric formulas can be represented into sum of two portions:

$$f_1(\vec{\boldsymbol{S}}_{(\ell)}) \triangleq g(\vec{\boldsymbol{S}}_{(\ell)}) + \varphi_1(\vec{\boldsymbol{S}}_{(\ell)}), \tag{3.5}$$

$$f_2(\vec{\boldsymbol{S}}_{(\ell)}) \triangleq g(\vec{\boldsymbol{S}}_{(\ell)}) + \varphi_2(\vec{\boldsymbol{S}}_{(\ell)}), \tag{3.6}$$

where g, φ_1 and φ_2 will be defined in Sections 3.2.1, 3.2.2 and 3.2.3, respectively. Notably, both metrics give the optimal performance. Their difference is mainly that the recursive computation of f_1 can be conducted by feeding the components of an OFDM symbol in a sequential fashion, while that of f_2 requires all the components at the same time; however, f_2 is more efficient since it expands less nodes during the priority-first search.

3.2.1 Recursive Maximum-Likelihood Metric g

By following a similar procedure to [3], we will derive the *recursive* ML metric g that can be used in the priority-first search algorithm. From (3.3), we obtain

$$\begin{aligned}
\hat{\vec{\boldsymbol{S}}} &= \arg\min_{\vec{\boldsymbol{S}}\in\mathcal{S}} \|\vec{\boldsymbol{X}} - \mathbb{P}_{\tilde{\boldsymbol{S}}}\vec{\boldsymbol{X}}\|^2 \\
&= \arg\min_{\vec{\boldsymbol{S}}\in\mathcal{S}} (\vec{\boldsymbol{X}} - \mathbb{P}_{\tilde{\boldsymbol{S}}}\vec{\boldsymbol{X}})^\dagger(\vec{\boldsymbol{X}} - \mathbb{P}_{\tilde{\boldsymbol{S}}}\vec{\boldsymbol{X}}) \\
&= \arg\min_{\vec{\boldsymbol{S}}\in\mathcal{S}} -\texttt{trace}(\mathbb{P}_{\tilde{\boldsymbol{S}}}\vec{\boldsymbol{X}}\vec{\boldsymbol{X}}^\dagger) \\
&= \arg\min_{\vec{\boldsymbol{S}}\in\mathcal{S}} -\texttt{trace}\left(\tilde{\boldsymbol{S}}(\tilde{\boldsymbol{S}}^\dagger\tilde{\boldsymbol{S}})^{-1}\tilde{\boldsymbol{S}}^\dagger\vec{\boldsymbol{X}}\vec{\boldsymbol{X}}^\dagger\right) \\
&= \arg\min_{\vec{\boldsymbol{S}}\in\mathcal{S}} -\texttt{trace}\left(\tilde{\boldsymbol{S}}\tilde{\boldsymbol{S}}^\dagger\vec{\boldsymbol{X}}\vec{\boldsymbol{X}}^\dagger\right) \quad \text{since } (\tilde{\boldsymbol{S}}^\dagger\tilde{\boldsymbol{S}})^{-1} = \frac{1}{2}\mathbb{I}_{\nu+1} \\
&= \arg\min_{\vec{\boldsymbol{S}}\in\mathcal{S}} -\texttt{trace}\left(\vec{\boldsymbol{S}}\mathbb{Q}_\nu\mathbb{Q}_\nu^\dagger\vec{\boldsymbol{S}}^\dagger\vec{\boldsymbol{X}}\vec{\boldsymbol{X}}^\dagger\right) \\
&= \arg\min_{\vec{\boldsymbol{S}}\in\mathcal{S}} -\texttt{trace}\left(\mathbb{Q}_\nu\mathbb{Q}_\nu^\dagger\vec{\boldsymbol{S}}^\dagger\vec{\boldsymbol{X}}\vec{\boldsymbol{X}}^\dagger\vec{\boldsymbol{S}}\right) \\
&= \arg\min_{\vec{\boldsymbol{S}}\in\mathcal{S}} -\texttt{vec}(\mathbb{Q}_\nu\mathbb{Q}_\nu^\dagger)^\dagger\texttt{vec}(\vec{\boldsymbol{S}}^\dagger\vec{\boldsymbol{X}}\vec{\boldsymbol{X}}^\dagger\vec{\boldsymbol{S}}).
\end{aligned} \tag{3.7}$$

In its detail, (3.7) can be written as

$$\hat{\vec{\boldsymbol{S}}} = \arg\min_{\vec{\boldsymbol{S}}\in\mathcal{S}} \left(-\sum_{m=1}^{N}\sum_{n=1}^{N}\delta_{m,n}\sum_{i=1}^{2}\sum_{j=1}^{2} S^*_{m,i}X_{m,i}S_{n,j}X^*_{n,j} \right) \tag{3.8}$$

where $S_{i,j}$ and $X_{i,j}$ are the components of $\vec{\boldsymbol{S}}$ and $\vec{\boldsymbol{X}}$, respectively, and $\delta_{m,n}$ is the (m,n)th entry of $(\mathbb{Q}_\nu\mathbb{Q}_\nu^\dagger)^T$. By denoting

$$w_{m,n} = \sum_{i=1}^{2}\sum_{j=1}^{2}\mathrm{Re}\{\delta_{m,n}S^*_{m,i}X_{m,i}S_{n,j}X^*_{n,j}\},$$

we obtain an equivalent expression of (3.8) as

$$\hat{\vec{\boldsymbol{S}}} = \arg\min_{\vec{\boldsymbol{S}}\in\mathcal{S}} \left[-2\sum_{m=1}^{N}\left(\sum_{n=1}^{m} w_{m,n} - \frac{1}{2}w_{m,m}\right)\right]. \tag{3.9}$$

A sufficient condition for the optimality of the priority-first search is that the path metric is *nondecreasing* along any path over the tree. To achieve this goal, we can add a constant $u_{m,n}$, independent of $\vec{\boldsymbol{S}}$, to (3.9) so that the metric becomes non-negative. According to the (3.9), a convenient choice that satisfies the need is $u_{m,n} = |w_{m,n}|$. By this, we know that for BPSK-modulated OFDM symbols,

$$u_{m,n} = \sum_{i=1}^{2}\sum_{j=1}^{2}|\mathrm{Re}\{\delta_{m,n}X_{m,i}X^*_{n,j}\}| \tag{3.10}$$

and for QPSK-modulated OFDM symbols,

$$u_{m,n} = \sum_{i=1}^{2}\sum_{j=1}^{2}|\delta_{m,n}X_{m,i}X^*_{n,j}|. \tag{3.11}$$

We then conclude the derivation as

$$\begin{aligned}\hat{\vec{\boldsymbol{S}}} &= \arg\min_{\vec{\boldsymbol{S}}\in\mathcal{S}} \left[2\sum_{m=1}^{N}\left(\sum_{n=1}^{m} u_{m,n} - \frac{1}{2}u_{m,m}\right) - 2\sum_{m=1}^{N}\left(\sum_{n=1}^{m} w_{m,n} - \frac{1}{2}w_{m,m}\right)\right] \\ &= \arg\min_{\vec{\boldsymbol{S}}\in\mathcal{S}} \left[\sum_{m=1}^{N}\left(\sum_{n=1}^{m} u_{m,n} - \frac{1}{2}u_{m,m}\right) - \sum_{m=1}^{N}\left(\sum_{n=1}^{m} w_{m,n} - \frac{1}{2}w_{m,m}\right)\right] \end{aligned} \tag{3.12}$$

Based on (3.12), we can define the metric g for every path $\vec{\boldsymbol{S}}_\ell$ over a tree to be

$$g(\vec{\boldsymbol{S}}_{(\ell)}) \triangleq \sum_{m=1}^{\ell}\left(\sum_{n=1}^{m} u_{m,n} - \frac{1}{2}u_{m,m}\right) - \sum_{m=1}^{\ell}\left(\sum_{n=1}^{m} w_{m,n} - \frac{1}{2}w_{m,m}\right), \tag{3.13}$$

which can be recursively computed via

$$g(\vec{\boldsymbol{S}}_{(\ell+1)}) \;=\; g(\vec{\boldsymbol{S}}_{(\ell)}) + \left(\sum_{n=1}^{\ell+1} u_{\ell+1,n} - \frac{1}{2}u_{\ell+1,\ell+1}\right) - \left(\sum_{n=1}^{\ell+1} w_{\ell+1,n} - \frac{1}{2}w_{\ell+1,\ell+1}\right). \tag{3.14}$$

3.2.2 The First Heuristic Function φ_1

We now derive the heuristic function in accordance with Lemma 2.1. Taking the ML metric g into the sufficient condition in (2.9) yields

$$\begin{aligned}&\sum_{m=1}^{\ell}\left(\sum_{n=1}^{m} u_{m,n} - \frac{1}{2}u_{m,m}\right) - \sum_{m=1}^{\ell}\left(\sum_{n=1}^{m} w_{m,n} - \frac{1}{2}w_{m,m}\right) + \varphi(\vec{\boldsymbol{S}}_{(\ell)})\\ &\quad\le \min_{\{\tilde{\vec{\boldsymbol{S}}}\in\mathcal{S}:\tilde{\vec{\boldsymbol{S}}}_\ell=\vec{\boldsymbol{S}}_\ell\}}\left[\sum_{m=1}^{N}\left(\sum_{n=1}^{m} u_{m,n} - \frac{1}{2}u_{m,m}\right) - \sum_{m=1}^{N}\left(\sum_{n=1}^{m} w_{m,n} - \frac{1}{2}w_{m,m}\right) + \varphi(\tilde{\vec{\boldsymbol{S}}})\right],\end{aligned} \tag{3.15}$$

where φ denotes the heuristic function. By noting that $\varphi(\tilde{\vec{\boldsymbol{S}}}) = 0$, the first heuristic function $\varphi = \varphi_1$ should satisfy

$$\begin{aligned}\varphi_1(\vec{\boldsymbol{S}}_{(\ell)}) \;\le\; &\min_{\{\tilde{\vec{\boldsymbol{S}}}\in\mathcal{S}:\tilde{\vec{\boldsymbol{S}}}_\ell=\vec{\boldsymbol{S}}_\ell\}}\left[\sum_{m=1}^{N}\left(\sum_{n=1}^{m} u_{m,n} - \frac{1}{2}u_{m,m}\right) - \sum_{m=1}^{N}\left(\sum_{n=1}^{m} w_{m,n} - \frac{1}{2}w_{m,m}\right)\right]\\ &-\left[\sum_{m=1}^{\ell}\left(\sum_{n=1}^{m} u_{m,n} - \frac{1}{2}u_{m,m}\right) - \sum_{m=1}^{\ell}\left(\sum_{n=1}^{m} w_{m,n} - \frac{1}{2}w_{m,m}\right)\right].\end{aligned} \tag{3.16}$$

If we demand that $\varphi_1(\vec{\boldsymbol{S}}_{(\ell)})$ is independent of the future routes of $\vec{\boldsymbol{S}}_{(\ell)}$, it is obvious that the all-zero heuristic function is the largest one that satisfies (3.16). Hence, we choose $\varphi_1(\vec{\boldsymbol{S}}_{(\ell)}) = 0$ for every $\vec{\boldsymbol{S}}_{(\ell)}$. This selection makes $f_1 = g + \varphi_1 = g$ on-the-fly computable. By simulations, the use of this metric in the priority-first search algorithm decreases the computational complexity in comparison with the straightforward exhaustive search.

3.2.3 The Second Heuristic Function φ_2

In comparison with f_1 (or φ_1) derived in the previous subsection, the computational complexity can be further reduced if we drop the requirement that the metric cannot depend on the future routes. Based on (3.16), we define

$$\begin{aligned}\varphi_2(\vec{\boldsymbol{S}}_{(\ell)}) \triangleq \; & \left[\sum_{m=1}^{N}\left(\sum_{n=1}^{m} u_{m,n} - \frac{1}{2}u_{m,m}\right) - \sum_{m=1}^{N}\left(\sum_{n=1}^{m} w_{m,n} - \frac{1}{2}w_{m,m}\right)\right] \\ & - \left[\sum_{m=1}^{\ell}\left(\sum_{n=1}^{m} u_{m,n} - \frac{1}{2}u_{m,m}\right) - \sum_{m=1}^{\ell}\left(\sum_{n=1}^{m} w_{m,n} - \frac{1}{2}w_{m,m}\right)\right]. \end{aligned} \tag{3.17}$$

We can simplify (3.17) to:

$$\varphi_2(\vec{\boldsymbol{S}}_{(\ell)}) \triangleq \sum_{m=\ell+1}^{N}\left(\sum_{n=1}^{m} u_{m,n} - \frac{1}{2}u_{m,m}\right) - \sum_{m=\ell+1}^{N}\left(\sum_{n=1}^{m} w_{m,n} - \frac{1}{2}w_{m,m}\right). \tag{3.18}$$

At the end of this subsection, we stress again that the trade-off between metrics f_1 and f_2 is that the recursion computation due to $f_1 = g$ in (3.14) requires only the next component, while adopting f_2 can yield a lower computational complexity.

3.3 The Maximum-Likelihood Demodulation Metric for the GLRT

For completeness, we also provide the maximum-likelihood demodulation metrics for the GLRT in this section. Similar to the discussion for the modified GLRT criterion in Section 3.2, two metric functions f_1 and f_2 will be introduced. With no ambiguity, we re-use the same notations g, f_1 and f_2 as those used in the previous section.

3.3.1 Recursive Maximum-Likelihood Metric g

We begin the derivation from (2.6) and obtain

$$\begin{aligned}
\hat{\vec{\boldsymbol{S}}} &= \arg\min_{\vec{\boldsymbol{S}}\in\mathcal{S}} \|\vec{\boldsymbol{X}} - \mathbb{P}_{\vec{\boldsymbol{S}}}\vec{\boldsymbol{X}}\|^2 \\
&= \arg\min_{\vec{\boldsymbol{S}}\in\mathcal{S}} \|\vec{\boldsymbol{X}} - \vec{\boldsymbol{S}}(\vec{\boldsymbol{S}}^\dagger\vec{\boldsymbol{S}})^{-1}\vec{\boldsymbol{S}}^\dagger\vec{\boldsymbol{X}}\|^2 \\
&= \arg\min_{\vec{\boldsymbol{S}}\in\mathcal{S}} -\texttt{trace}\left((\vec{\boldsymbol{S}}^\dagger\vec{\boldsymbol{S}})^{-1}\vec{\boldsymbol{S}}^\dagger\vec{\boldsymbol{X}}\vec{\boldsymbol{X}}^\dagger\vec{\boldsymbol{S}}\right) \\
&= \arg\min_{\vec{\boldsymbol{S}}\in\mathcal{S}} -\texttt{trace}\left(\vec{\boldsymbol{S}}^\dagger\vec{\boldsymbol{X}}\vec{\boldsymbol{X}}^\dagger\vec{\boldsymbol{S}}\right) \quad \text{since } (\vec{\boldsymbol{S}}^\dagger\vec{\boldsymbol{S}}) = 2\mathbb{I}_{\nu+1} \\
&= \arg\min_{\vec{\boldsymbol{S}}\in\mathcal{S}} -\texttt{vec}\,(I)\,\texttt{vec}\left(\vec{\boldsymbol{S}}^\dagger\vec{\boldsymbol{X}}\vec{\boldsymbol{X}}^\dagger\vec{\boldsymbol{S}}\right). \qquad (3.19)
\end{aligned}$$

In its detail, (3.19) can be written as

$$\hat{\vec{\boldsymbol{S}}} = \arg\min_{\vec{\boldsymbol{S}}\in\mathcal{S}} -\sum_{m=1}^{N}\sum_{i=1}^{2}\sum_{j=1}^{2} S_{m,i}^* X_{m,i} S_{m,j} X_{m,j}^*. \qquad (3.20)$$

Similar to the derivation in Section 3.2.1, we add a constant so as to make the resultant metric nondecreasing along the paths over the tree:

$$\hat{\vec{\boldsymbol{S}}} = \arg\min_{\vec{\boldsymbol{S}}\in\mathcal{S}} \left(\sum_{m=1}^{N}\sum_{i=1}^{2}\sum_{j=1}^{2} |X_{m,i}X_{m,j}^*| - \sum_{m=1}^{N}\sum_{i=1}^{2}\sum_{j=1}^{2} S_{m,i}^* X_{m,i} S_{m,j} X_{m,j}^*\right). \qquad (3.21)$$

The above formula is suitable for both BPSK- and QPSK-modulated OFDM symbols. In light of (3.21), the ML metric function used in the priority-first search can be defined as

$$g(\vec{\boldsymbol{S}}_{(\ell)}) \triangleq \sum_{m=1}^{\ell}\sum_{i=1}^{2}\sum_{j=1}^{2} |X_{m,i}X_{m,j}^*| - \sum_{m=1}^{\ell}\sum_{i=1}^{2}\sum_{j=1}^{2} S_{m,i}^* X_{m,i} S_{m,j} X_{m,j}^*. \qquad (3.22)$$

Accordingly, its recursive form is given by

$$g(\vec{\boldsymbol{S}}_{(\ell+1)}) = g(\vec{\boldsymbol{S}}_{(\ell)}) + \sum_{i=1}^{2}\sum_{j=1}^{2} |X_{\ell+1,i}X_{\ell+1,j}^*| - \sum_{i=1}^{2}\sum_{j=1}^{2} S_{\ell+1,i}^* X_{\ell+1,i} S_{\ell+1,j} X_{\ell+1,j}^* \qquad (3.23)$$

As anticipated, the g function just derived for the GLRT is less complicated than its counterpart for the modified GLRT in (3.14).

3.3.2 The First Heuristic Function φ_1

By following similar procedure to Section 3.2.2, the heuristic function for the GLRT should satisfy

$$\sum_{m=1}^{\ell}\sum_{i=1}^{2}\sum_{j=1}^{2}|X_{m,i}X_{m,j}^*| - \sum_{m=1}^{\ell}\sum_{i=1}^{2}\sum_{j=1}^{2} S_{m,i}^* X_{m,i} S_{m,j} X_{m,j}^* + \varphi(\vec{\boldsymbol{S}}_{(\ell)})$$
$$\leq \min_{\{\tilde{\vec{\boldsymbol{S}}}\in\mathcal{S}:\tilde{\vec{\boldsymbol{S}}}_\ell=\vec{\boldsymbol{S}}_\ell\}} \left[\sum_{m=1}^{N}\sum_{i=1}^{2}\sum_{j=1}^{2}|X_{m,i}X_{m,j}^*| - \sum_{m=1}^{N}\sum_{i=1}^{2}\sum_{j=1}^{2} S_{m,i}^* X_{m,i} S_{m,j} X_{m,j}^* + \varphi(\tilde{\vec{\boldsymbol{S}}})\right] \quad (3.24)$$

So the choice $\varphi(\vec{\boldsymbol{S}}_{(\ell)}) = \varphi_1(\vec{\boldsymbol{S}}_{(\ell)}) = 0$ results in the desired f_1, which is required to be independent of the future receptions.

3.3.3 The Second Heuristic Function φ_2

Again, by relaxing the requirement that the heuristic function should be independent of the future receptions, we can define the second heuristic function φ_2 according to (3.24) as:

$$\varphi_2(\vec{\boldsymbol{S}}_{(\ell)}) \triangleq \sum_{m=\ell+1}^{N}\sum_{i=1}^{2}\sum_{j=1}^{2}|X_{m,i}X_{m,j}^*| - \sum_{m=\ell+1}^{N}\sum_{i=1}^{2}\sum_{j=1}^{2} S_{m,i}^* X_{m,i} S_{m,j} X_{m,j}^*. \quad (3.25)$$

Similar to the situation for the modified GLRT, the selection φ_2 helps lowering the computational complexity when it is compared with φ_1.

Chapter 4

Simulation Results

In this chapter, we will examine the Modified GLRT by simulations. Specifically, the simulation results are summarized in Section 4.1, and their corresponding discussions are given in Section 4.2.

4.1 System Settings

In Sections 2.2 and 3.1, we have mentioned that half of the transmission bits should be fixed as specified in (2.8). We however did not explain why they are so chosen and what the differences are for other choices.

Figures 4.1–4.5 summarize the performances and demodulation complexities of alternative assignments for these fixed bits. By taking $N = 6$ as an example, the notation "2222" in these figures represents that $S_{1,\mathbf{2}}S_{2,\mathbf{2}}S_{3,\mathbf{2}}S_{4,\mathbf{2}}S_{5,\mathbf{2}}S_{6,\mathbf{2}}$ are chosen fixed instead. Similarly, "2211" and "2121" indicate that $S_{1,\mathbf{2}}S_{2,\mathbf{2}}S_{3,\mathbf{2}}S_{4,\mathbf{1}}S_{5,\mathbf{1}}S_{6,\mathbf{1}}$ and $S_{1,\mathbf{2}}S_{2,\mathbf{1}}S_{3,\mathbf{2}}S_{4,\mathbf{1}}S_{5,\mathbf{2}}S_{6,\mathbf{1}}$ are chosen fixed, respectively. It can then be observed that different assignments only have negligible influence on the performance and demodulation complexity. We thus use the bit assignment "2121" in the following simulations.

Similar to [3], in these figures, the demodulation complexity is measured by the average path expansions per information bit. This kind of measurement is generally considered to be proportional to the average number of metric calculations per information bit. In Tables 4.1 and 4.2, the detailed correspondence of the metric calculation to additions and multiplications are provided. It indicates from the two tables that this usual measure, i.e., the average node expansions per information, does not completely reflect the execution speed of a decoding algorithm. Usually, the Modified GLRT requires more operations than the GLRT and metric f_2 is more complex than metric f_1.

Figure 4.6 illustrates the BER performances of the BPSK-OFDM systems. The corresponding demodulation complexities with metrics f_1 and f_2, respectively, are summarized in Figures 4.7 and 4.8.

The BERs of the QPSK-OFDM systems are then given in Figure 4.9. Its respective demodulation complexities are provided in Figure 4.10.

Finally, Figure 4.11 compares the BER performances of BPSK- and QPSK-OFDM systems that are demodulated by the Modified GLRT.

The discussions regarding these figures will be given in the next section.

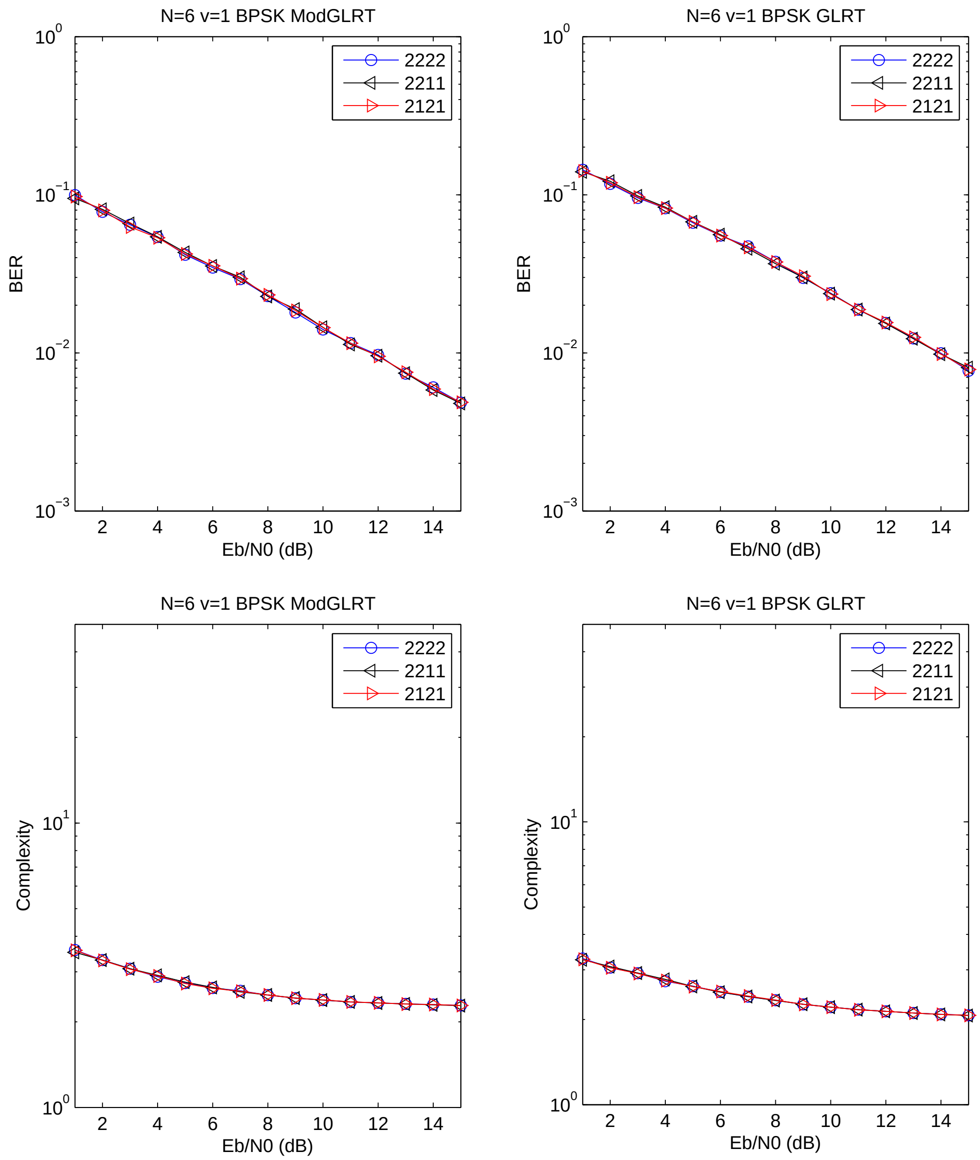

Figure 4.1: The BERs and demodulation complexities of different 3 bit assignments with BPSK transmission symbols demodulated by the Modified GLRT and the GLRT, respectively. Here, $N = 6$ and $\nu = 1$.

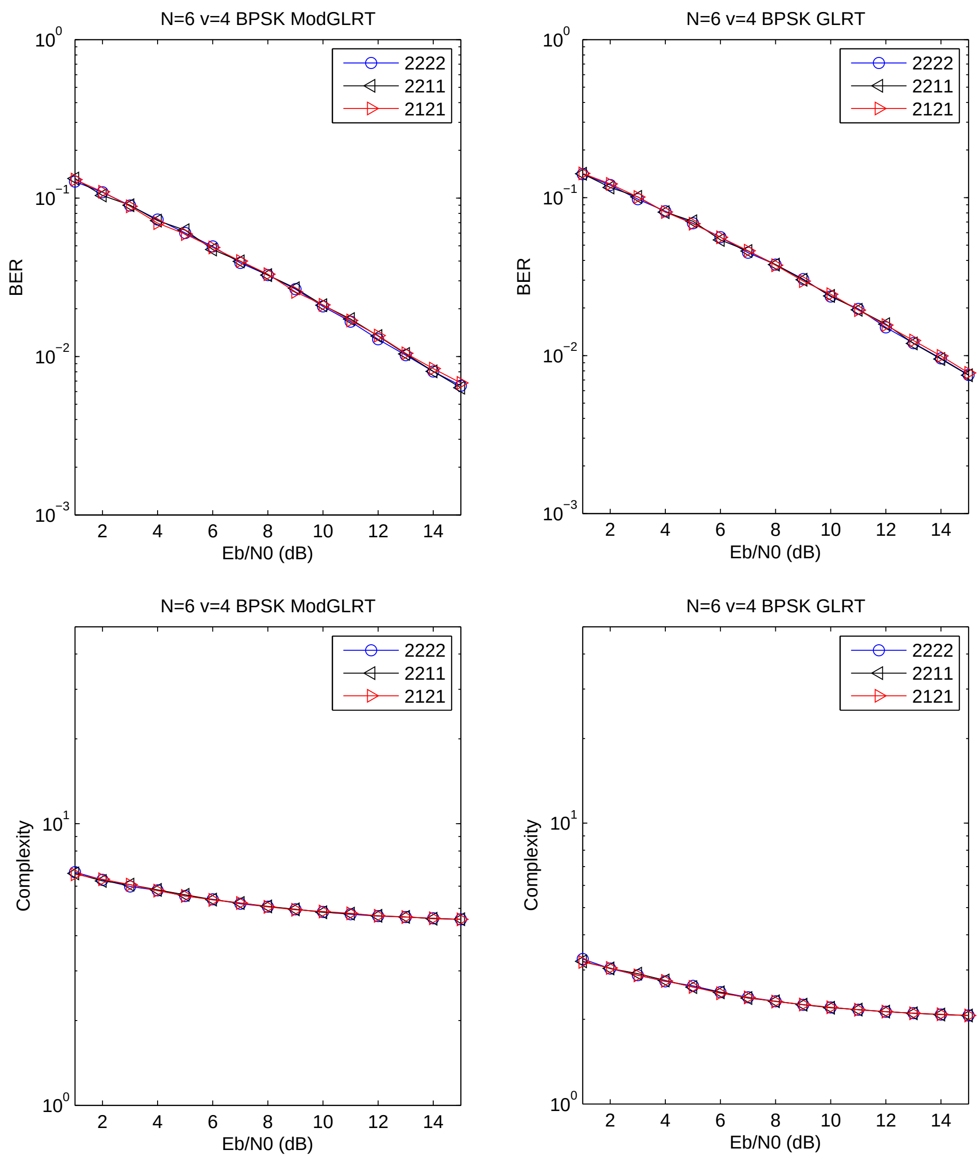

Figure 4.2: The BERs and demodulation complexities of 3 bit assignments with BPSK transmission symbols demodulated by the Modified GLRT and the GLRT, respectively. Here, $N = 6$ and $\nu = 4$.

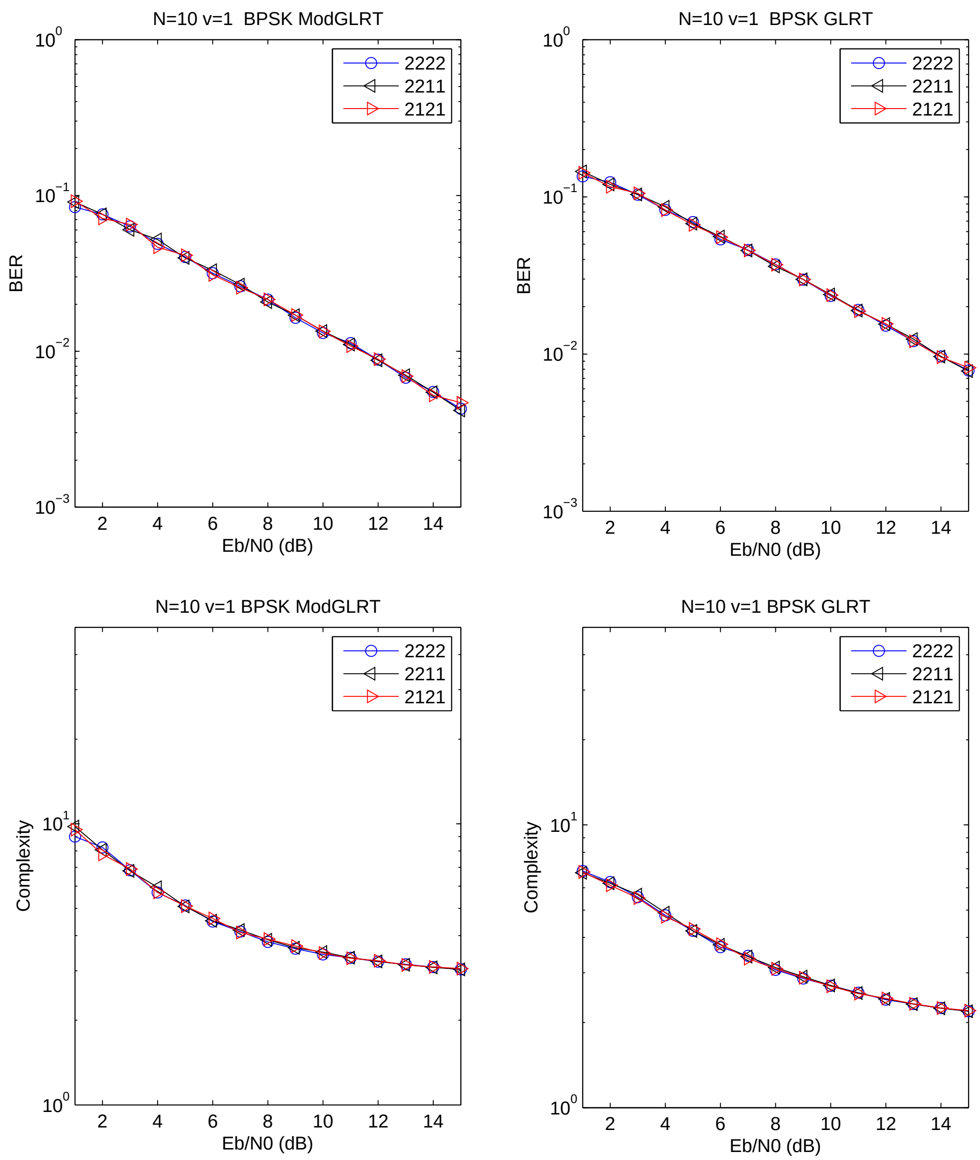

Figure 4.3: The BERs and demodulation complexities of different 3 bit assignments with BPSK transmission symbols demodulated by the Modified GLRT and the GLRT, respectively. Here, $N = 10$ and $\nu = 1$.

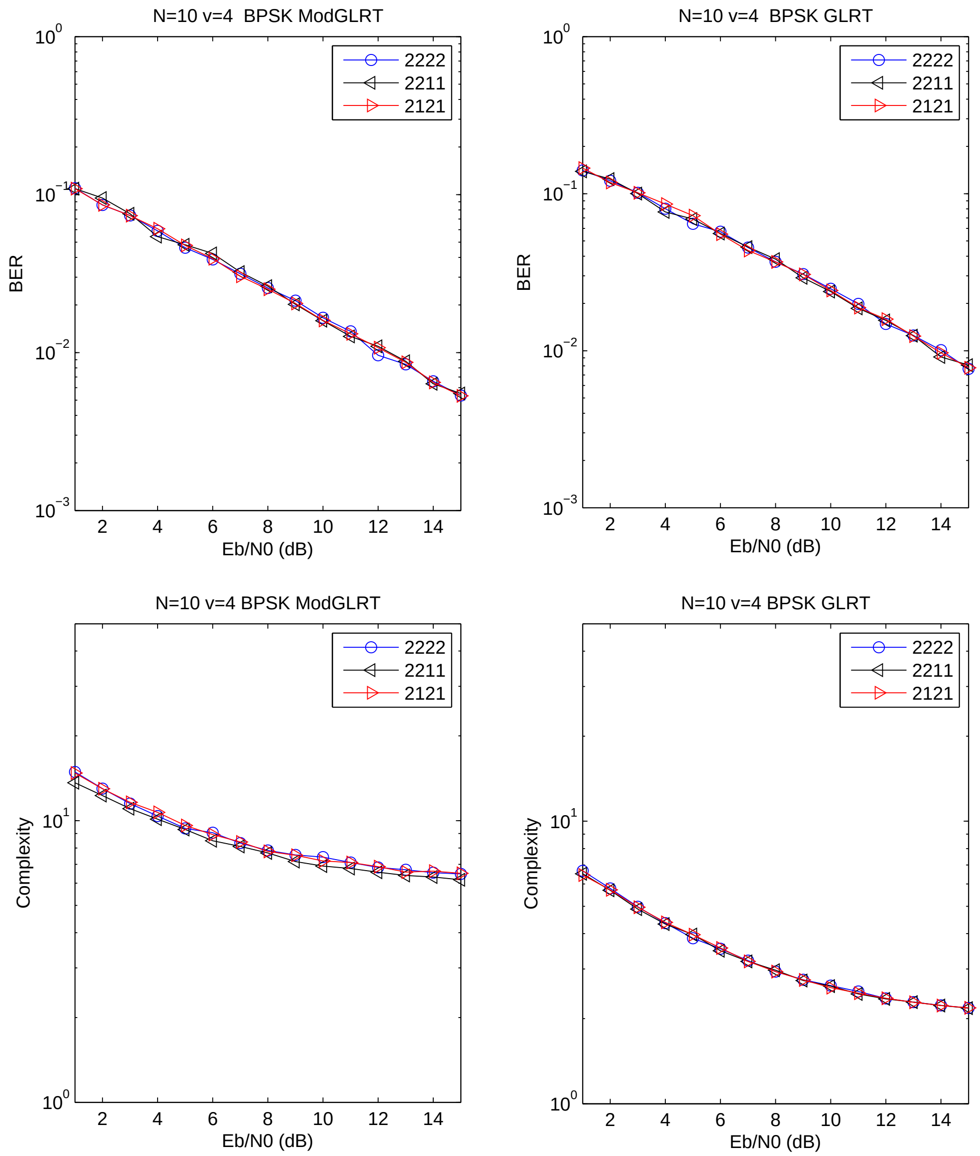

Figure 4.4: The BERs and demodulation complexities of different 3 bit assignments with BPSK transmission symbols demodulated by the Modified GLRT and the GLRT respectively. Here, $N = 10$ and $\nu = 4$.

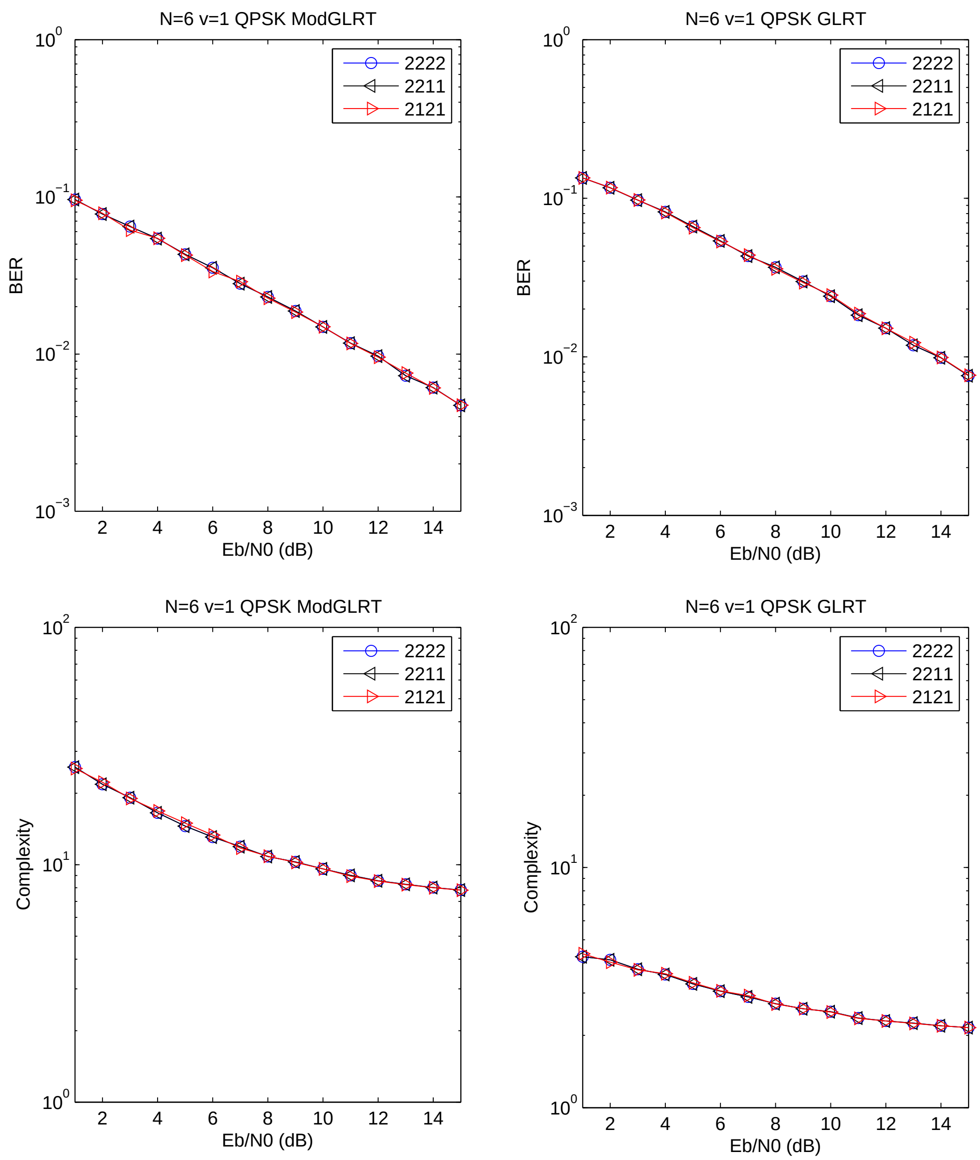

Figure 4.5: The BERs and demodulation complexities of different 3 bit assignments with QPSK transmission symbols demodulated by the Modified GLRT and the GLRT respectively. Here, $N = 6$ and $\nu = 1$.

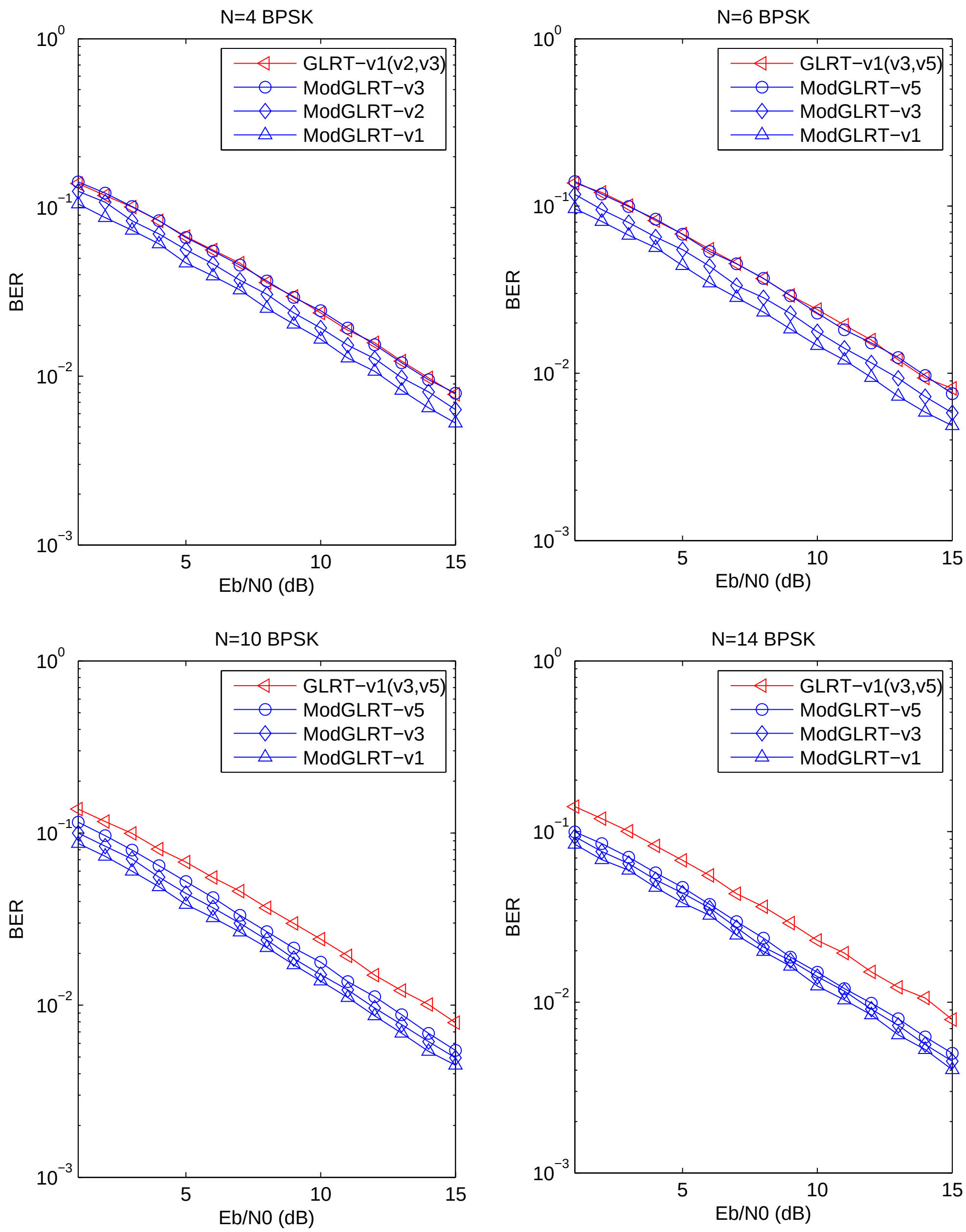

Figure 4.6: The BERs of the BPSK-OFDM systems demodulated by the Modified GLRT and the GLRT, respectively. The lengths examined are $N = 4, 6, 10, 14$.

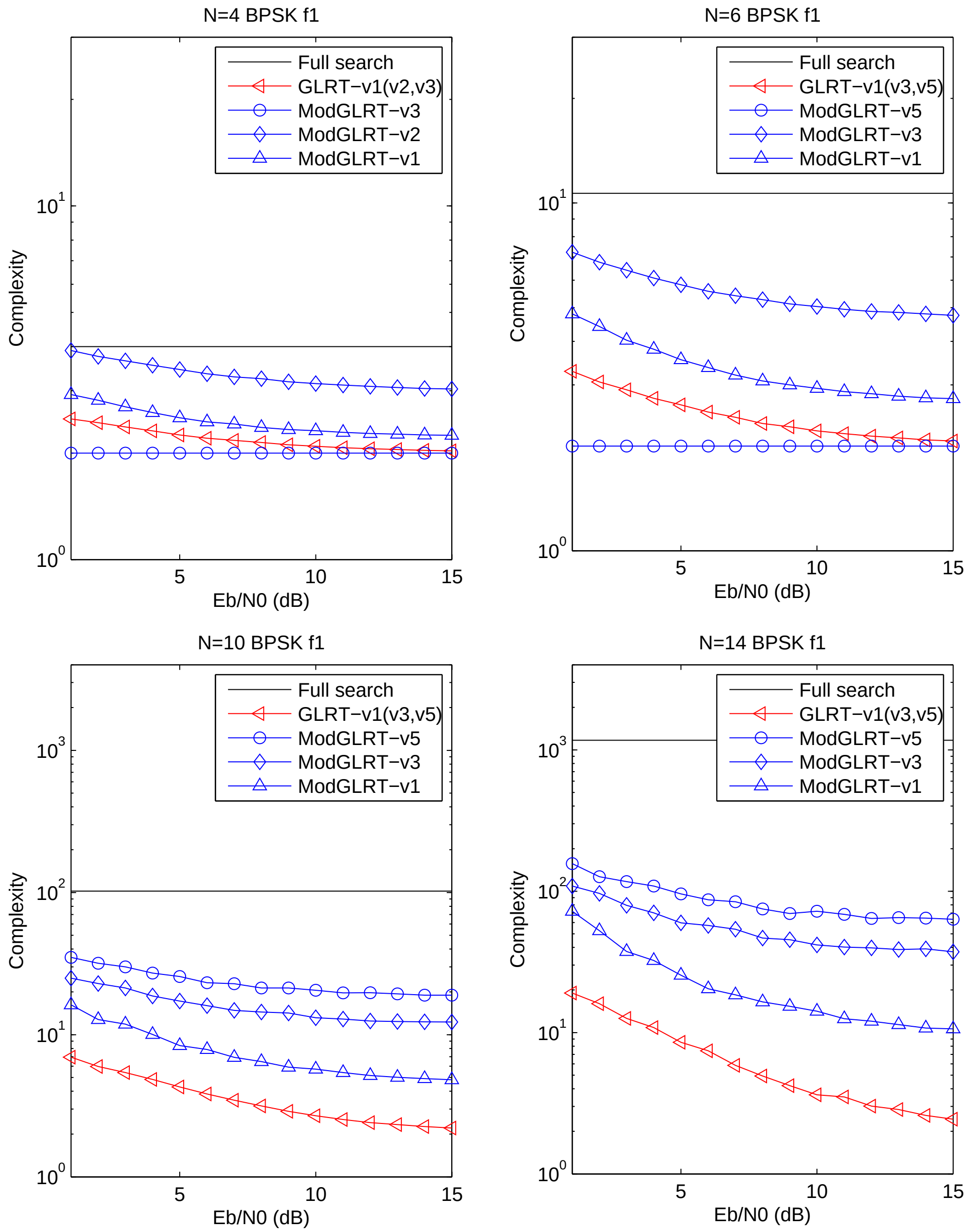

Figure 4.7: The demodulation complexities corresponding to Figure 4.6, using the demodulation metric f_1

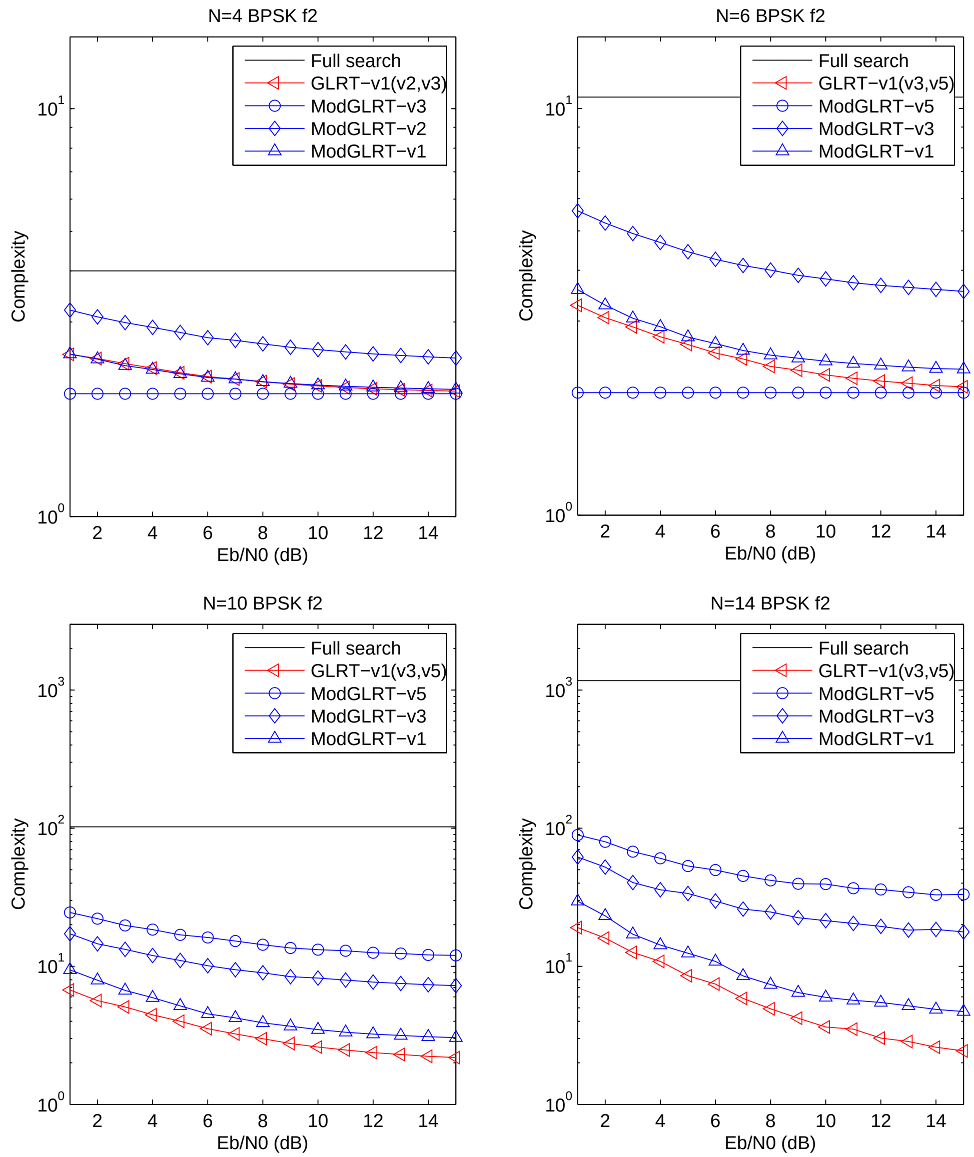

Figure 4.8: The demodulation complexities corresponding to Figure 4.6, using the demodulation metric f_2

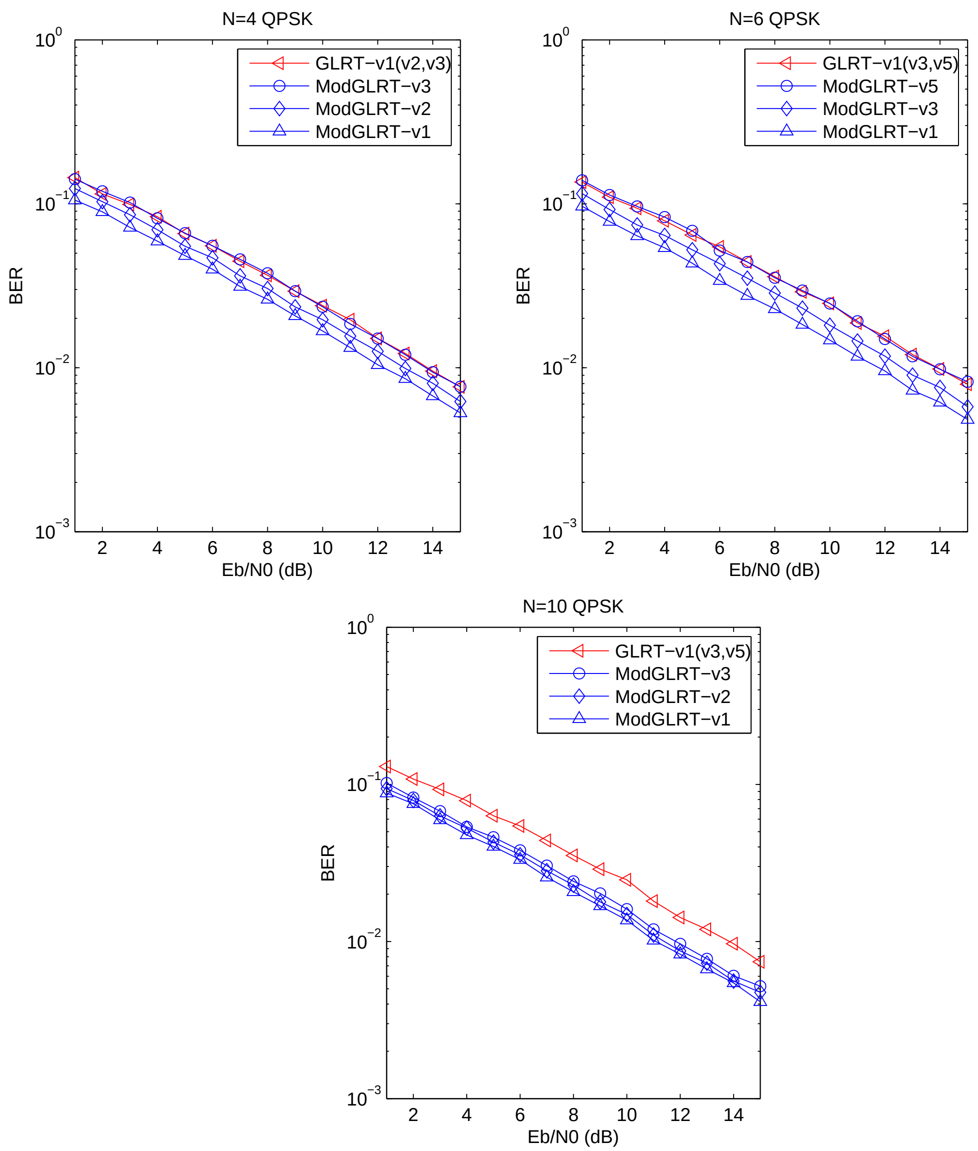

Figure 4.9: The BERs of the QPSK-OFDM systems demodulated by the Modified GLRT and the GLRT, respectively. The lengths examined are $N = 4, 6, 10$.

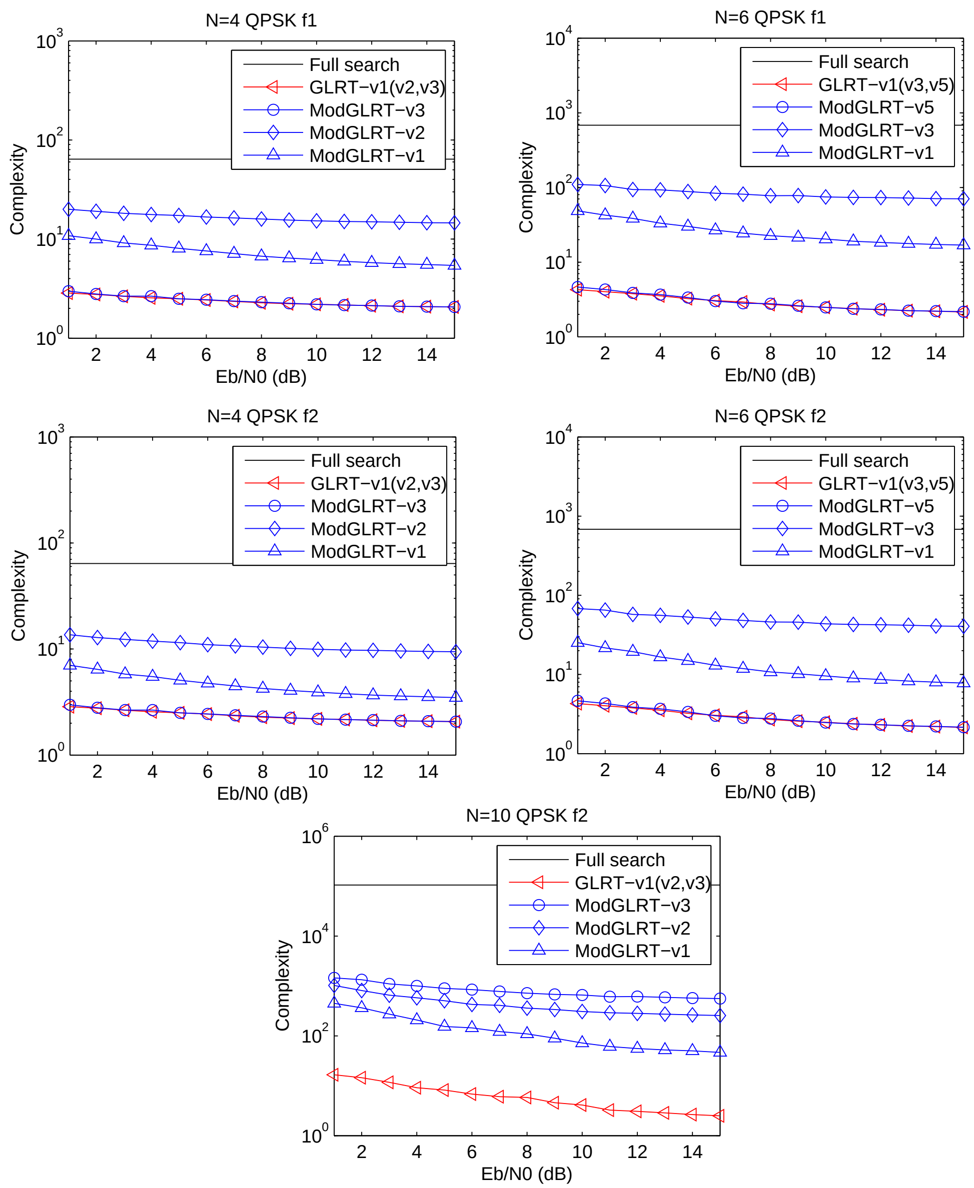

Figure 4.10: The demodulation complexities corresponding to Figure 4.9, using the demodulation metrics f_1 and f_2

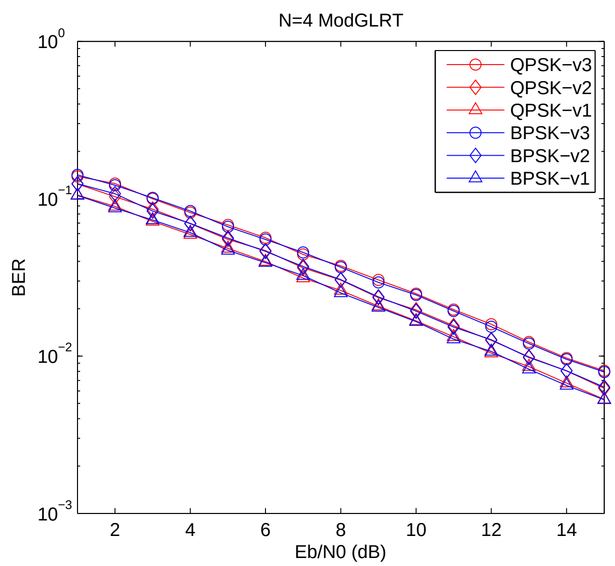

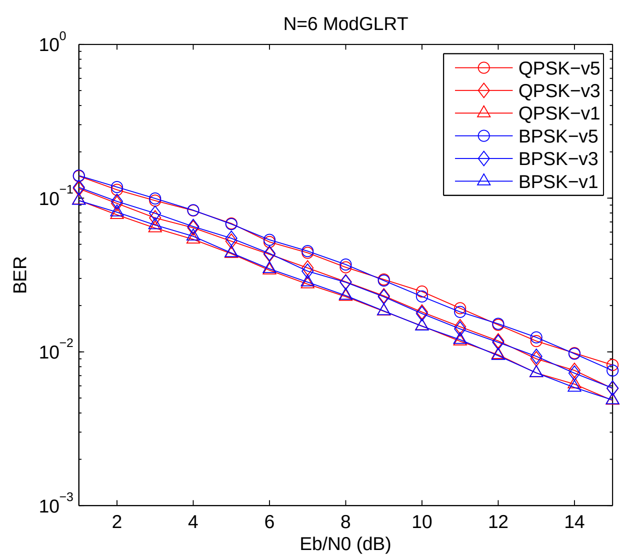

Figure 4.11: The BERs of the BPSK-OFDM and QPSK-OFDM systems demodulated by the Modified GLRT. The lengths examined are $N = 4, 6$.

4.2 Observations and remarks

From Figures 4.6 and 4.9, it can be observed that when N is fixed, the BERs of the Modified GLRT increase as ν grows. Take the $N = 6$ BPSK-OFDM system as an example. The case of $\nu = 5$ requires extra 2.2 dB transmission power to achieve BER=10^{-2} when it is compared with the case of $\nu = 1$. These figures also show that the BERs of the Modified GLRT are always below those of the GLRT, for which the performance remains unchanged for different ν. In the special case that $\nu = N - 1$ (for example, $N = 4, \nu = 3$ and $N = 6, \nu = 5$), the performances of the Modified GLRT and the GLRT are identical. This is consistent with what have been proved in Lemma 3.1.

In Figure 4.11, the BERs of the BPSK-OFDM and the QPSK-OFDM systems demodulated by the Modified GLRT are examined, and are shown to have comparable performances.

Next we turn to the decoding complexities. We first look at those cases that $\nu \neq N - 1$. From Figures 4.7, 4.8 and 4.10, we observe that the demodulation complexities of the Modified GLRT are always larger than that of the GLRT, no matter which of the metrics f_1 and f_2 is implemented. Besides, when N is fixed, the demodulation complexities of the Modified GLRT increases significantly with ν. For example, when metric f_2 is considered under the $N = 14$ BPSK-OFDM system, the number of average node expansions approximately equals 5 for $\nu = 1$ but increases to 30 for $\nu = 5$ at SNR=15 dB. A final observation for the cases of $\nu \neq N - 1$ is that the demodulation complexities can be greatly reduced when metric f_2 is employed instead of metric f_1. For example, for the $N = 14$ BPSK-OFDM system, adopting metric f_2 results in only 33 node expansions while it requires 63 node expansions for metric f_1 at SNR=15 dB.

Regarding the special case of $\nu = N - 1$, we found that the two decoding metrics f_1 and f_2 are identical because φ_2 is zero; so both metrics will yield the same decoding complexities. A striking observation for this special case is that the Modified GLRT has an evidently lower demodulation complexity than the GLRT, and can actually achieve the minimum node expansions (i.e., two node expansions) per information bit when BPSK-OFDM systems are adopted. When QPSK-OFDM systems are employed instead, the demodulation complexities of the Modified GLRT are the same as the GLRT since the demodulation metrics of both demodulation schemes are identical at $\nu = N - 1$.

	additions for f_1	multiplications for f_1
GLRT	7	16
Modified GLRT	$8\ell + 1$	$24\ell + 2$

Table 4.1: Numbers of operations required for calculating metric f_1 for a node expansion at level ℓ

	additions of f_2	multiplications of f_2
GLRT	$7(N - \ell + 1)$	$16(N - \ell + 1)$
Modified GLRT	$4(N^2 + 3N - \ell^2 - \ell)$	$12(N^2 + 3N - \ell^2 - \ell) + 4$

Table 4.2: Numbers of operations required for calculating metric f_2 for a node expansion at level ℓ

Chapter 5

Conclusion Remarks and Future Work

In this thesis, we proposed the Modified GLRT criterion for blind demodulation of the OFDM signals transmitted over a frequency-selective channel. As anticipated, the proposed Modified GLRT demodulator can jointly perform channel estimation and data correction. By deriving the recursive formula corresponding to the Modified GLRT criterion, we can apply the priority first search algorithm to the Modified GLRT, and hence the demodulation complexity is significantly reduced in comparison with the exhaustive demodulator. By simulations, we found that the BER performance can be improved by using the Modified GLRT demodulator when it is compared with the GLRT demodulator.

As for the future work, we mainly put effort in the OFDM system based on BPSK and QPSK modulations in this thesis. However, it should be interesting to examine our Modified GLRT demodulation for the QAM-modulation-based OFDM system, which is of more common use in OFDM system and which can provide a higher data rate. In addition, although the demodulation complexity of the Modified GLRT is reduced by introducing the priority-first search, the complexity still grows exponentially with respect to the symbol length N. Efforts should be placed to further reduce the demodulation complexity without sacrifice much of the good performance of the Modified GLRT.

Bibliography

[1] O. Shayevitz and M. Feder, "Universal decoding for frequency-selective fading channels," *IEEE Trans. Inf. Theory*, vol. 51, no. 8, pp. 2770-2790, August 2005.

[2] M. Skoglund, J. Giese and S. Parkvall, "Code design for combined channel estimation and error protection," *IEEE Trans. Inf. Theory*, vol. 48, no. 5, pp. 1162-1171, May 2002.

[3] C.-L. Wu, P.-N. Chen, Yunghsiang S. Han and M.-Hsin Kuo, "Maximum-likelihood priority-first search decodable codes for combined channel estimation and error protection," *IEEE Trans. Inf. Theory*, vol. 55, no. 9, pp. 4191-4203, Sept. 2009.

[4] T. Cui, "Joint data detection and channel estimation for OFDM systems," *IEEE Trans. Commun.*, vol. 54, no. 4, pp. 670-679, April 2006.

[5] J. Proakis, *Digital Communications*, McGraw-Hill, fifth edition, 2007.

[6] S. Haykin, *Communication Systems*, Wiley, fourth edition, 2001.

[7] D. Tse, *Fundamentals of Wireless Communication*, Cambridge University Press, fourth edition, 2005.

[8] S M. Kay, *Fundamentals of Statistical Signal of Processing, vol.2 : Detection Theory*, Prentice Hall PTR, 1998.

[9] N. Seshadri, “Joint data and channel estimation using blind trellis search techniques,” *IEEE Trans. Commun.* , vol. 42, no. 2/3/4, pp. 1000-1011, February/March/April 1994.